Tormentic acid, a triterpenoid compound isolated from the fruits of Chaenomeles speciose, protected indomethacin-induced gastric mucosal lesion via modulating miR-139 and CXCR4/CXCL12/PLC/PKC/Rho A/MLC pathway

Junyu He
China Three Gorges University
Adeline Ngeng Ngwa
China Three Gorges University
Yuanyuan Zhang
China Three Gorges University
Haibo He (hjy219@126.com)
China Three Gorges University
Yumin He
China Three Gorges University
Daoxiang Xu
Seventh People's Hospital of Wenzhou
Xiao Wang
China Three Gorges University
Jie Li
China Three Gorges University
Jihong Zhang
China Three Gorges University
Guofan Xu
University of Aberdeen
Junzhi Wang
China Three Gorges University
Kun Zou
China Three Gorges University

Research Article

Keywords: fruits of Chaenomeles speciose, tormentic acid, gastric mucosal lesion, cell proliferation and migration, CXCR4/CXCL12/PLC/PKC/Rho A/MLC pathway

Posted Date: May 9th, 2022

DOI: https://doi.org/10.21203/rs.3.rs-1616587/v1

Tormentic acid, a triterpenoid compound isolated from the fruits of *Chaenomeles speciose*, protected indomethacin-induced gastric mucosal lesion via modulating miR-139 and CXCR4/CXCL12/PLC/PKC/Rho A/MLC pathway

Junyu He[1]†, Adeline Ngeng Ngwa[2]†, Yuanyuan Zhang[2], Haibo He[2,3,*], Yumin He[1], Daoxiang Xu[4,*], Xiao Wang[2], Jie Li[2], Jihong Zhang[5], Guofan Xu[6], Junzhi Wang[2] and Kun Zou[2]

[1] College of Medical Science, China Three Gorges University, Yichang, Hubei, 443002, PR China

[2] Yichang Key Laboratory of Development and Utilization of Health Products with Drug Food Homology, Hubei Key Laboratory of Natural Products Research and Development, China Three Gorges University, Yichang, Hubei, 443002, PR China

[3] Hubei Key Laboratory of Tumor Microenvironment and Immunotherapy, College of Medical Science, China Three Gorges University, Yichang, Hubei, 443002, PR China

[4] Seventh People's Hospital of Wenzhou, Wenzhou, Zhejiang, 325005, PR China

[5] Chinese Medicine Clinical Medical College, China Three Gorges University, Yichang 443002, PR China

[6] Business School, University of Aberdeen, Aberdeen AB15 5EY, United Kingdom

Junyu He and Adeline Ngeng Ngwa contributed equally to this work

Corresponding authors: Haibo He, hjy219@126.com

Daoxiang Xu, xdx.2006@163.com

Address: Hubei Key Laboratory of Natural Products Research and Development, China Three Gorges University, 8, University Avenue, Yichang 443002, PR China; Seventh People's Hospital of Wenzhou, 552, Shanxi East Road, Wenzhou 325005, PR China.

Running title: Tormentic Acid Protecting Gastric Lesion

Abstract

Our previous study demonstrated that pentacyclic triterpenoids from the fruits of *Chaenomeles speciosa* had prominent treatment functions on gastric damage patients and animals. However, little has been known about the pharmacological activity and mechanism of its each triterpene component (oleanolic acid, maslinic acid, betulinic acid, ursolic acid, 3-O-acetyl ursolic acid, 3-O-acetyl pomolic acid, tormentic acid (TA)). In current study, we found that TA possessed stronger cell protective effect and promoted proliferation activity on IND-damaged GES-1 cells than other triterpenoids from the fruits of *Chaenomeles speciose* by bioscreening. Therefore, we selected TA for further research. The results demonstrated that TA might ameliorate the gastric mucosal injury induced by IND, which was associated with accelerating the damaged GES-1 cell proliferation and migration, meliorating the injured rat GBF, ulcer inhibitor, ulcer area and pathologic changes of gastric mucous tissue, reducing the total acidity and volume of the gastric effluents, and raising the gastric pH; Further empirical research indicated that TA dramatically suppressed miR-139 mRNA expression, elevated CXCR4 and CXCL12 mRNA and protein expressions, p-PLC, p-PKC, Rho A, MLCK and p-MLC protein expressions. these data demonstrated that TA avoided gastric mucosal injury by suppressing miR-139 expression and activating the CXCR4/CXCL12/PLC/PKC/Rho A/MLC pathway, thereby boosting the epithelial cell proliferation and migration, and promoting the gastric damaged healing.

Keywords: fruits of *Chaenomeles speciose*; tormentic acid; gastric mucosal lesion; cell proliferation and migration; CXCR4/CXCL12/PLC/PKC/Rho A/MLC pathway

Introduction

With the change of modern life style, environmental pollution and irrational use of non-steroidal anti-inflammatory drugs (NSAIDs), gastrointestinal mucosal lesion has become one of the major diseases that seriously endanger public health and social development, causing great economic and social burden to all countries in the world, especially in the developing countries (Namulema et al. 2018; Malley 2003). As gastric mucosal lesion is the main pathophysiological link of gastric ulcer, gastritis and many other gastric diseases, it is also recognized by WHO as the inevitable mode of inducing gastric ulcer, chronic gastritis, atrophic gastritis, and finally developing into gastric cancer (Da et al. 2019). Therefore, it has important clinical significance to protect gastric mucosa and promote the healing of damaged gastric mucosa for the treatment of gastric diseases and prevention of further deterioration (Aihara et al. 2017). In the damaged gastric mucosa, the reconstruction of gastrointestinal barrier can be mediated by collective migration, proliferation and subsequent differentiation of epithelial cells (Hoffmann 2005). This process is achieved by activating the normal epithelial cells migration around the lesion to the injured area, which can be divided into rapid repair and slow repair: the former refers to the migration of intact epithelial cells around the damaged mucosa to the damaged mucosal surface, so that the damaged epithelium can recover continuity and integrity quickly; the latter is the process of cell proliferation, is to compensate damaged or necrotic mucosal cells through the mitosis and differentiation of the cells themselves, the organism covers the injured area or around the lesion through inflammatory response, cell mitosis and differentiation, and new cell migration, so that the damaged gastric mucosal tissue returns to normal (Liu et al. 2018; Engevik et al. 2019; Cho and Mills 2019). Therefore, the proliferation and migration of gastric epithelial cells is of great significance in promoting the healing of damaged gastric mucosa.

MicroRNAs (miRs) are a class of non-coding single stranded RNA molecules, which participate in multiple pathophysiological processes, such as migration, proliferation, differentiation, angiogenesis and so forth (Chen et al. 2018). Recent evidence manifests that miR-139 is extensively touched on the pathological processes of digestive system lesions and tumors, Alzheimer's disease and myocardial injury (Wang et al. 2021). Zhang and his colleagues (Zhang et al. 2018) indicated that miR-139 might negatively modify the CXC motif chemokine receptor 4 (CXCR4) expression, regulate CXCR4/CXC motif chemokine ligand 12 (CXCL12) signal axis, and then inhibit the

migration and proliferation of breast cancer MDA-MB-231 cells. Simultaneously, our previous studies also identified that the gastric mucosal protection of total triterpenoids from the fruits of *Chaenomeles speciose* was linked with suppressing miR-139 expression, and activating CXCR4/CXCL12 pathway (Qin et al. 2016a; He et al. 2017b).It's always been known that CXCR4 is a specific receptor for CXCL12, composed of 352 amino acids, which is a protein receptor expressed on different types of cells seven times across the membrane (Hwang et al. 2012). Smith and his colleagues (Smith et al. 2005) demonstrated that CXCL12 signaling through CXCR4 stimulated epithelial cell migration, reconstructed mucosal barrier, and repaired the damaged gastric mucosa. Whereas, phospholipase C (PLC) is a target downstream of CXCR4 and a class of enzymes existed on the cytoplasmic membrane that can hydrolyze phospholipids, which plays a role in mediating cell signal transduction by triggering PLC/protein kinase C (PKC) signal cascade (Croitoru et al. 2016). Rho A is a small molecule G protein that regulates cell migration, infiltration and metastasis through the reorganization of the cytoskeleton, and is related to cell growth and differentiation by regulating the growth cycle of cells (Cherfils and Zeghouf 2013; Rathinam et al. 2011). Myosin light chain kinase (MLCK) is a serine/threonine protein kinase that exists in mammals, and belongs to the family of calmodulin-dependent protein kinases, participates in many important life activities (Liu et al. 2018). Aihara, Hwang and their research teams (Aihara et al. 2017; Hwang et al. 2012) found that trifoliate factor might directly or indirectly activate CXCR4 in epithelial cells, and then transmit signals and produce effects in sequence by triggering PLC/PKC signal cascade and phosphorylation of amino acid residues. On the one hand, it could activate intracellular calcium dependent signal transduction by increasing the driving force of extracellular Ca^{2+} influx, impel the conversion of Rho A from inactive GDP binding form to active GTP binding form and activate Rho kinase, and enhance MLCK activity to stimulate MLC phosphorylation, raise the formation of actin stress fibers, and induce epithelial cell migration; On the other hand, it could also stimulate E-cadherin relocation and monolayer tightening through Rho associated protein kinase (ROCK) activation and actin recombination, restore the function of mucosal barrier, and then accelerate the repair of damaged mucosa. Through the above analysis, it is not difficult for us to find out that miR-139 and CXCR4/CXCL12/PLC/PKC/Rho A/MLC pathway assume a critical role in facilitating the healing of damaged gastric mucosa. Therefore, the targeted miR-139 and

CXCR4/CXCL12/PLC/PKC/Rho A/MLC pathway will offer a new idea for the treatment of gastric lesion.

The fruits of *Chaenomeles speciosa* (Sweet) Nakai, or “Mugua”, has the effect of relaxing meridians and activating collaterals, harmonizing stomach and resolving dampness, which traditionally been used to treat dampness arthralgia, severe pain of waist and knee joint, heat dampness vomiting and diarrhea, muscle contracture pain, beriberi edema, etc (China Pharmacopoeia Committee 2020). we had reported that the ethyl acetate extract of *Chaenomeles speciosa* fruit and its active pentacyclic triterpenoid constituents exhibited positively therapeutic effects on patients and animals with gastric mucosal injury (Qin et al. 2015; Qin et al. 2016; He et al. 2017; Rodríguez et al. 2003; Nam et al. 2006). A tide of research indicated that pentacyclic triterpenoids had a wide range of pharmacological activities, and single pentacyclic triterpenoids (such as oleanolic acid) have anti-inflammatory, antioxidant activities and gastric mucosal protective effects, but its activity is mainly anti-inflammatory and antioxidant (Ishikawa et al. 2008); If the number or species of pentacyclic triterpenoids increased (e.g., niga-ichigoside F1 and 23-hydroxyformic acid) or species elevated (e.g., Oleanolic acid, ursolic acid, betulinic acid, 3-O-acetyl ursolic acid, 3-O-acetyl pomolic acid, maslinic acid, tormentic acid (TA)), its protective effect on gastrointestinal mucosa was significantly enhanced compared with single pentacyclic triterpenoids, and their anti-inflammatory and antioxidant activities are continuously retained (Qin et al. 2016a, He et al. 2017b; da Rosa et al. 2018; Gomes et al. 2009; Pan et al. 2018). We have previously reported that the pentacyclic triterpenoids from the fruits of *Chaenomeles speciose* mainly included oleanolic acid, maslinic acid, betulinic acid, ursolic acid, 3-O-acetyl ursolic acid, 3-O-acetyl pomolic acid, TA and so on (Shi et al. 2016). However, little has been known about the pharmacological activity and mechanism of its each triterpene component. Therefore, in the current study, we first screened the triterpenoid compound with the best gastroprotective activity in pentacyclic triterpenoids from the fruits of *Chaenomeles speciose*, and then further investigated its gastroprotective effects on the damaged GES-1 cells and rats induced by IND and potential mechanisms by adjusting miR-139-mediated CXCR4/CXCL12/PLC/PKC/RhoA/ MLC pathway.

Materials and methods

Experimental material

Oleanolic acid, ursolic acid, betulinic acid, 3-O-acetyl ursolic acid, 3-O-acetyl pomolic acid, maslinic acid, TA (Fig. 1A) used in this study were isolated from the fruits of *Chaenomeles speciose* (Sweet) Nakai as previously described (Shi et al. 2016). The aforementioned isolated compounds were determined by liquid chromatography-mass spectrometry and found to be over 95% pure. The fruits of *Chaenomeles speciosa* (Sweet) Nakai were harvested from Ziqiu Mugua Planting Base (Yichang, China) and identified by professor Yubing Wang. The voucher specimens (2021-0745) are preserved in Yichang Key Laboratory of Development and Utilization of Health Products with Drug Food Homology, China Three Gorges University.

Reagents

All reagents such as medium, trypsin, PBS, DMSO, MTT, Annexin V-FITC/Propidium Iodide (PI), Hoechst 33258, JC-1, and so forth used for the cell culture and experiment in the research were purchased from BD Biosciences (Bedford, MA, USA); Lactate dehydrogenase (LDH) was purchased from Hefei Laier Biotechnology Co., Ltd (Hefei, China); Bestar Real-time PCR RT and Bestar TM Real-time PCR kits were purchased from DBI Bioscience Corporation (Ludwigshafen, Ger); Dual Luciferase Reporter Assay System were obtained from Promega Corporation (Madison, WI, USA); Trizol isolation kit was obtained from Invitrogen Corporation (Carlsbad, CA, USA); miR-139 mimic, miR-139 inhibitor, miR mimic negative control (mimic NC), inhibitor negative control (inhibitor NC), siRNA of CXCR4 (CXCR4 si RNA) and negative siRNA (siRNA NC) were obtained from GenePharma Company (Shanghai, China); Lipofectamine 3000 reagent was purchased from Invitrogen Corporation (Carlsbad, CA, USA); Primary antibodies (CXCR4, CXCL12, PLC, p-PLC, PKC, p-PKC, Rho A, MLCK, MLC, p-MLC) were obtained from Cell Signaling Technology (Danvers, MA, USA); WesternBright ECL prime detection reagent, SDS-PAGE gel kit, PVDF membrane were procured from Mingyang Kehua Biotechnology Co., Ltd (Beijing, China).

Cell culture and transfection

Human gastric mucosal epithelial cells (GES-1) were used as a gift from Professor Hongfeng Gu from Nanhua University and grown in RPMI-1640 medium containing 10% FBS at 37 °C in a humidified 5% CO_2 atmosphere, which were inoculated in a 6-well plate to adhere for 24 h, then GES-1 cells were transfected miR-139 mimic, miR-139 inhibitor, CXCR4 si RNA or scrambled

miR NC for 24 h. The detailed methods were carried out in the light of our previous description (He et al. 2020).

Viability assay

After GES-1 cells (1×10^5 cells/well) were inoculated in a 96-well plate to adhere for 24 h, preprocessing with oleanolic acid, ursolic acid, betulinic acid, 3-O-acetyl ursolic acid, 3-O-acetyl pomolic acid, maslinic acid and TA (1.563, 3.125、6.25、12.5、25、50 μM) for 6 h, then added IND (700 μM) to damage GES-1 cells and continuously cultured for 18 h according to our previous description (Qin et al. 2016a). The viability assays were estimated by MTT method. Their viability analysis of GES-1 cells pretreated with TA (12.5 μM) used alone or combined with miR-139 mimic, miR-139 inhibitor, CXCR4 siRNA were also similar with it.

LDH leakage assay

After GES-1 cells (300 cells/well) were inoculated in a 6-well plate to adhere for 24 h, their treatment methods were the same as "viability assay". The supernatant of each well was collected, and the LDH leakage was determined using assay kit. Their LDH leakage assays of GES-1 cells pretreated with TA (12.5 μM) used alone or combined with miR-139 mimic, miR-139 inhibitor, CXCR4 siRNA were also similar with it.

Colony formation assay

The adherent GES-1 cells (300 cells/well) inoculated in 6-well plates were treated with TA (12.5 μM) used alone or combined with the miR-139 mimics, miR-139 inhibitor and CXCR4 siRNA. The medium was changed every 3 days. 18 h before the end of the experiment, the final concentration of 700 μM IND was added to each group except the control group. After 14 days of culture, colony formation assay was performed according to our previous description (He et al. 2020).

Wound healing assay

After GES-1 cells (1×10^5 cells/well) transfected with miR-139 mimic, miR-139 inhibitor or CXCR4 siRNA were inoculated in a 24-well plate to adhere for 24 h, the scratch-wounds were formed by scraping the cultured cell of every culture plate with a 200-μL micropipette tip. After the floating cells were removed by using PBS washing, TA (12.5 μM) was added, and continued to culture for 6 h, added 700 μM IND except for the control group, and then unceasingly cultured. The

wound healing assay was carried out at 0, 12 and 24 h respectively in the light of our previous description (He et al. 2020).

Migration assay

After GES-1 cells (5×10^4 cells/well) transfected with miR-139 mimic, miR-139 inhibitor or CXCR4 siRNA were inoculated on the upper chamber of the plate, the lower chamber was filled with 10% FBS medium which contained IND (700 μM) and/or TA (12.5 μM) as the control group, IND group, TA (12.5 μM) groups, respectively. After cultured in a 37°C incubator for 24 h, the upper chamber was taken out, and rinsed twice with PBS, fixed by methanol, stained with 0.1% crystal violet, and then observed and photographed under a Olympus microscope (Tokyo, Japan). Cells from five random fields per filter were counted using Image J software system (Bethesda, MD, USA).

Hoechst staining

After GES-1 cells (1×10^5 cells/well) transfected with miR-139 mimic, miR-139 inhibitor or CXCR4 siRNA were inoculated in a 6-well plate to adhere for 24 h, TA (12.5 μM) was added, and continued to culture for 6 h, added 700 μM IND except for the control group, and then unceasingly cultured. After 18 h of continuous culture, Hoechst staining was performed in the light of our previous description (He et al. 2020).

Annexin V-FITC/PI cytometric assay

After GES-1 cells (1×10^5 cells/well) transfected with miR-139 mimic, miR-139 inhibitor or CXCR4 siRNA were inoculated in a 6-well plate to adhere for 24 h, TA (12.5 μM) was added, and continued to culture for 6 h, added 700 μM IND except for the control group, and then unceasingly cultured. After 18 h, the apoptosis was detected by using the Annexin V-FITC/PI dying method according to a previous description (He et al. 2020).

Mitochondrial viability assay

After GES-1 cells (1×10^5 cells/well) transfected with miR-139 mimic, miR-139 inhibitor or CXCR4 siRNA were inoculated in a 6-well plate to adhere for 24 h, TA (12.5 μM) was added, and continued to culture for 6 h, added 700 μM IND except for the control group, and then unceasingly cultured. After 18 h, the mitochondria viability was tested with JC-1 kit in the light of a previous description (Qin et al. 2016a).

Luciferase reporter assay

The connected site in the 3'-UTR of CXCR4 was elaborated by PCR, and implanted the the pmir GLO Luciferase miRNA Target Expression Vector (Promega, USA), it was termed a CXCR4 wild type (CXCR4-WT). The connected sites were substituted for forming the negative control: CXCR4 mutated type (CXCR4-MUT). The vectors were transfected with miR-139 mimic or the mimic NCs with Lipofectamine 3000 reagent. After being transfected for 48 h, the luciferase activities were detected.

Animal, establishment of mice gastric mucosal damage model and treatments

Male Sprague-Dawley rats (six-week old) were procured form the Laboratory Animal Center of China Three Gorges University (Yichang, China), which were feeded in a 12 h light/dark cycle and temperature and humidity regulated surroundings. During the experiment the rats were allowed ad libitum to feed and water, and experimental procedures were carried out according to the guiding principle of the National Institutes of Health (Bethesda, USA). The experimental scheme was ratified by the Laboratory Animal Care and Use Committee of China Three Gorges University (CTGUEAC-2021-079)

The rat model of gastric mucosal lesion was established according to our previous description (Qin et al. 2016a). Specific method was as follows: After a week of adaptation, the rats were randomized into five groups with 20 rats in each group including control, IND, TA-L (1 mg/kg) + IND, TA-M (2 mg/kg) + IND and TA-H (4 mg/kg) + IND groups. The experimental rats in each TA groups were administrated previously with TA once a day for 21 continuous days, and rats in the control group and IND group were administrated with a vehicle (0.5% carboxymethylcellulose sodium) of the same volume. After the last administration, the rats were deprived of food but allowed to drink freely. All groups except the control group were given IND (100 mg/kg) by gavage after 24 h. The experiment was implemented on the 2 h and 6 h after IND, respectively.

Gastric juice parameter determination

2 h After administrated IND, the pylorus of 10 rats randomized in each group were ligatured, meanwhile, their waters were also deprived. The experimental rat was anaesthetized with 20% chloral hydrate (1.2 g/kg, *i.p.*) after pylorus ligation for 4 h. Their abdominal cavities were opened, the stomach were dislodged, and then cut open along the greater curvature of the stomach, the gastric contents were collected. The Gastric juice volume, pH value and total acidity were detected as the described methods by Dhiyaaldeen *et al* (Dhiyaaldeen et al. 2014).

Gastric ulcer analysis

After collected stomach's contents, the stomachs were flushed with icy normal saline, and then photographed. The ulcer area and inhibition rate were totalled according to our early description (He et al. 2020). After taking pictures of the stomachs, the gastric tissue samples were selected for morphological analysis and molecular biology experiments.

GBF detection

6 h After administrated IND, The remaining rats in each group were anesthetized, and the stomach incisions were made on the anterior gastric wall along the greater curvature for detecting the gastric blood flow (GBF) by the Laser Doppler Flowmeter (Vasamedics, USA) as the described method by Magierowski *et al* (Magierowski et al. 2017).

Gastric wall mucus content measurement

After monitoring GBF, the rat's stomach was moved out, the mucus content of gastric wall was determined in the light of the described method by Dhiyaaldeen *et al* (Dhiyaaldeen et al. 2014).

Histopathology analysis

Gastric tissues were fixed, sectioned and stained, and then the sections were evaluated according to the criteria established by Laine and Weinstein (Laine and Weinstein 1988), and comments were blind.

Quantitative real-time polymerase chain reaction (qRT-PCR) analysis

The total RNAs were isolated from GES-1 cells and gastric tissue by using Trizol kit (Invitrogen, USA). Then, they were reversed transcription into cDNAs. miRNA and mRNA expressions were quantified using SYBR Green real-time PCR Master Mix kits. U6 and GAPDH were acted as the internal controls for miRNAs and mRNA, respectively. The primer sequences used in qRT-PCR were set out in Table 1, and synthesized by solarbio science & technology co., ltd (Beijing, China).

Western blotting analysis

The total proteins of the GES-1 cells and gastric tissues were extracted with protein isolation kits. The protein concentration was measured by automatic nucleic acid detector (Thermo scientific, USA). The protein expressions of CXCR4, CXCL12, PLC, p-PLC, PKC, p-PKC, Rho A, MLCK, MLC, p-MLC in GES-1 cells and gastric tissues were measured with western blotting analysis, which was executed in the light of our previous description (Qin et al. 2016a; Qin et al. 2016b).

Statistical analysis

SPSS statistics 21.0 software was used for statistical analysis, and the data were expressed as mean ± SD. Student's t-tests were used for data analysis between the two groups, and Tukey test in one-way ANOVA was used for data analysis between multiple groups. $P<0.05$ was considered to be statistically significant.

Results

The pentacyclic triterpenoids from the fruits of *Chaenomeles speciose* (Sweet) Nakai promoted IND-injuried cell proliferation and suppressed LDH leakage

To evaluate the influences of the pentacyclic triterpenoids (oleanolic acid, maslinic acid, betulinic acid, ursolic acid, 3-O-acetyl ursolic acid, 3-O-acetyl pomolic acid and TA) from the fruits of *Chaenomeles speciose* (Sweet) Nakai on the cytotoxicity and proliferation of the GES-1 cells damaged by IND, the cells were treated with oleanane-type triterpenoids (oleanolic acid and maslinic acid), lupane-type triterpenoids (betulinic acid) and ursane-type triterpenoids (ursolic acid, 3-O-acetyl ursolic acid, 3-O-acetyl pomolic acid and TA) (1.563-50 μM) on the IND-injuried GES-1 cells for 24 h, respectively. Compared to IND-injuried group, oleanolic acid (25 μM), maslinic acid (25 μM), betulinic acid (12.5, 25 μM), ursolic acid (12.5, 25, 50 μM), 3-O-acetyl ursolic acid (6.25, 12.5, 25 μM), 3-O-acetyl pomolic acid (25, 50 μM) and TA (3.125, 6.25, 12.5 μM) significantly promoted the IND-injuried cell proliferation ($P<0.05$ or $P<0.01$, respectively); While their proliferative activities were dramatically inhibited with the increase of their concentrations ($P<0.05$ or $P<0.01$, respectively) (Fig. 1B-D).

Furthermore, cell damage could also be indirectly evaluated by LDH leakage, the more injuried a cell is, the more it leaks. So its leakage rate from cytoplasm into the medium is the important indicator of demonstrating the integrity of cell membrane and the degree of cell damage (Wang et al. 2019). In order to further survey the protective effects of the pentacyclic triterpenoids (oleanolic acid, maslinic acid, betulinic acid, ursolic acid, 3-O-acetyl ursolic acid, 3-O-acetyl pomolic acid and TA), the LDH release rates under their intervention were evaluated. As indicated in Fig. 1E-G, a remarkable elevation of LDH leakage from cytoplasm into the medium was detected in the IND-injuried group, and the LDH leakage topped out at 30 folds in contrast to the control group ($P<0.01$). In contrast, oleanolic acid (25 μM), maslinic acid (25 μM), betulinic acid (12.5, 25 μM), ursolic acid (12.5, 25, 50 μM), 3-O-acetyl ursolic acid (6.25, 12.5, 25 μM), 3-O-acetyl pomolic acid (25, 50 μM)

and TA (3.125, 6.25, 12.5 μM) treatments prominently restrained the IND-damaged cell LDH leakage in contrast to the IND group (P<0.05 or P<0.01, respectively). Based on the existing study, TA among the pentacyclic triterpenes from the fruits of *Chaenomeles speciose* (Sweet) Nakai and its appropriate concentrations (under 12.5 μM) were selected for further study.

TA promoted IND-injuried GES-1 cell proliferation and restrained apoptosis

Niv and Banić (Niv and Banić 2014) demonstrated that restraining the apoptosis of gastric mucosal epithelial cells and promoting their proliferations were the prerequisite for promoting the repair of damaged gastric mucosa. After assessing the influences of the pentacyclic triterpenoids and the safe concentration range of TA, we further investigated its effects on the proliferation and apoptosis of IND-injuried GES-1 cells in the pretreatment with TA used alone or combined using the miR-139 mimics and miR-139 inhibitor. As indicated in Fig. 2A and Fig. 3A, C, E, the proliferative activities of the IND-injuried or combined transfection with miR-139 mimic GES-1 cells were dramatically suppressed, mitochondrial viabilities were reduced, and apoptosis were elevated in contrast to the control or mimic NC group (P<0.01, respectively). TA used alone or combined using the miR-139 mimics obviously facilitated IND-injuried GES-1 cell proliferation, raised mitochondrial viabilities and suppressed apoptosis in contrast to the IND or mimic NC group (P<0.01, respectively). Interestingly, transfection with miR-139 inhibitor or combination using TA or TA used alone dramatically accelerated IND-injuried GES-1 cell proliferation, elevated mitochondrial viabilities and suppressed apoptosis in contrast to the IND or inhibitor NC group (P<0.01, respectively) (Fig. 2B and Fig. 3B, D, F). The aforementioned data indicated that the anti-apoptotic and pro-proliferative effects of TA were relation to suppressing miR-139 expression.

TA boosted IND-injuried GES-1 cell migration

The gastric epithelium is an important part of the gastric mucosal barrier, which is an essential part in renovating the injuried gastric mucosa and preserving mucosal structural integrity. After gastric mucosal damage, the migration and proliferation of adjacent gastric mucosal epithelial cells is an important way to complete this process (Aihara et al. 2018). After accomplishing the analysis of TA promoting GES-1 cell proliferation, we further researched its effect on IND-impaired GES-1 cell migration by wound healing and Transwell assays, respectively. As demonstrated in Fig. 4A and C, the migration activities of the IND-injuried or combined using the miR-139 mimics GES-1 cells were significantly depressed in contrast to the control or mimic NC group (P<0.01,

respectively). TA used alone or combined using the miR-139 mimics obviously accelerated IND-damaged GES-1 cell migration in contrast to the IND or mimic NC group (P<0.01, respectively). In contract, transfection with miR-139 inhibitor or combination using TA or TA used alone prominently boosted IND-injuried GES-1 cell migration in contrast to the IND or inhibitor NC group (P<0.01, respectively) (Fig. 4B and D). The data demonstrated that the potential migration-promoting activity of TA, which was relation to repressing miR-139 expression in IND-injuried GES-1 cells.

TA facilitated the IND-injuried GES-1 cell migration via suppressing miR-139 expression and activating CXCR4/CXCL12/PLC/PKC/Rho A/MLC pathway

The aforementioned results demonstrated the protective effect of TA was linked with facilitating the IND-impaired GES-1 cell migration. To confirm whether miR-139 was concerned in the migration effects of TA on IND-impaired GES-1 cells, we detected the miR-139 expression. As manifested Fig. 5A, the miR-139 mRNA expression in IND-impaired GES-1 cells was notably promoted in contrast to the control group (P<0.01), and the mRNA expression level of miR-139 further elevated in the miR-139 mimic-transfected GES-1 cells in contrast to the mimic NC group (P<0.01). Instead, IND-impaired GES-1 cells and miR-139 mimic-transfected IND-impaired GES-1 cells pretreated with TA (12.5 μM) exhibited dramatically reduced miR-139 expressions in contrast to the IND and mimic NC groups (P<0.01, respectively). The current results were coincident with TA accelerating IND-impaired GES-1 cell migration in wound healing and Transwell assays (Fig. 4A and C), which demonstrated that the cytoprotective and migration-promoting effects of TA was relation to restraining miR-139 expression.

Aihara and Hwang *et al* (Aihara et al. 2017; Hwang et al. 2012) found that CXCR4/ CXCL12/PLC/PKC/Rho A/MLC pathway played the fundamental role in ameliorating the impaired gastric mucosal repair and healing. To illustrate this, the protein expression assay of this pathway was performed in the miR-139 mimic-transfected IND-impaired GES-1 cells. As manifested Fig. 5B and C, the CXCR4, CXCL12 mRNA and protein expressions and p-PLC, p-PKC, Rho A, MLCK and p-MLC protein expressions in IND-impaired GES-1 cells were dramatically reduced in contrast to the control group (P<0.01); After the IND-impaired GES-1 cells transfected with miR-139 mimic, the above-mentioned protein expressions were further revised down sharply in the miR-139 mimic-transfected GES-1 cells in contrast to the mimic NC group (P<0.01). In contract, TA (12.5 μM)

used alone or combined using the miR-139 mimics markedly elevated the CXCR4, CXCL12 mRNA and protein expressions and p-PLC, p-PKC, Rho A, MLCK and p-MLC protein expression levels in contrast to the IND or mimic NC group (P<0.01, respectively). There were no obvious changes in the protein expressions of PLC, PKC and MLC after administration of TA used alone or combined using miR-139 mimic.

miR-139 knockdown reinforced the activating effect of TA on CXCR4/CXCL12/PLC/ PKC/Rho A/MLC signaling pathway by targeting the CXCR4 gene

In order to further verify whether miR-139 was stretched to the IND-impaired GES-1 cell migration, we tested the GES-1 cell viability, apoptosis and detected migration, miR-139 expression and CXCR4/CXCL12/PLC/PKC/Rho A/MLC pathway related protein expressions after the IND-injuried GES-1 cells were omitted miR-139 gene by transfecting with miR-139 inhibitor or combined with TA or TA used alone. As the Fig. 2B, Fig. 3B, D, F, Fig. 4B, D and Fig. 6A indicated, the knockdown of miR-139 or combined with TA or TA used alone significantly facilitated the cell proliferation, migration, raised mitochondrial viability, pushed down apoptosis and miR-139 expression in the IND-impaired cells or miR-139 inhibitor-transfected IND-damaged GES-1 cells in contrast to the IND or inhibitor NC group. Simultaneously, western blotting analytical results also manifested that the CXCR4/CXCL12/ PLC/PKC/Rho A/MLC pathway was impacted greatly in the miR-139 inhibitor-transfected IND-impaired GES-1 cells. As indicated in Fig. 6B, C, the CXCR4, CXCL12 mRNA and protein expressions and p-PLC, p-PKC, Rho A, MLCK and p-MLC protein expression levels were distinctly raised in the miR-139 inhibitor-transfected IND-damaged GES-1 cells in contrast to the IND or inhibitor NC group. Interestingly, pretreatment with TA (12.5 μM) used alone or combined using the miR-139 inhibitor further elevated the CXCR4, CXCL12 mRNA and protein expressions and p-PLC, p-PKC, Rho A, MLCK and p-MLC protein expressions in contrast to the IND group or inhibitor NC group (P<0.01, respectively).

Based on the above, we found that miR-139 had a negative regulatory effect on CXCR4 of IND-impaired GES-1 cells. Notwithstanding, whether CXCR4 is the prospective target gene of miR-139 is not yet known. To verify this, we predicted it by the prediction software of miRecords website database. As demonstrated in Fig. 7A, CXCR4 was forecasted to be a extrapolated target gene of miR-139. To further demonstrate, the dual luciferase reporter gene assay was executed after transfected with WT or MUT 3’ -UTR sequence of CXCR4 combined using mimic NC or miR-139

mimic in GES-1 cells. The results indicated that transfection with miR-139 mimic apparently reduced the luciferase activity co-transfected with WT 3’-UTR of CXCR4, but aroused no influence on luciferase activity in MUT 3′-UTR of CXCR4 (Fig. 7B). Concurrently, we also discovered that the CXCR4 mRNA and protein expressions were substantially suppressed by miR-139 mimic, and substantially improved by miR-139 inhibitor or combined using TA or TA used alone in GES-1 cells (Fig. 7C-E). Consequently, CXCR4 was the target gene of miR-139, and the knockdown of miR-139 or pretreatment with TA effectively activated CXCR4/CXCL12/ LC/PKC/Rho A/MLC pathway.

CXCR4 knockdown attenuated the cytoprotection and migration of TA against IND-damaged GES-1 cells

In order to intensify the evidence connecting TA cytoprotection and migration are related to CXCR4, CXCR4 siRNA was transfected in GES-1 cells by knocking down the CXCR4 expression. Fig. 8A and B demonstrated that the CXCR4 mRNA and protein expressions in GES-1 cells were apparently cut down by CXCR4 siRNA transfection in contrast to the siRNA NC and control groups (P<0.01, respectively). In IND-impaired GES-1 cells, transfection with CXCR4 siRNA obviously reduced GES-1 cell proliferation, migration, mitochondrial viabilities, facilitated apoptosis and miR-139 expression in contrast to the IND group (P<0.01, respectively). After pretreatment with TA, the aforementioned suppressed quotas and elevated apoptosis and miR-139 expression were noticeably reversed in IND-impaired GES-1 cells in contrast to CXCR4 siRNA group (P<0.01, respectively) (Fig. 8C-G and Fig. 9A-C). Furthermore, qRT-PCR and western blot results also demonstrated that the CXCR4 knockdown apparently weakened the CXCR4, CXCL12 mRNA and protein expressions and p-PLC, p-PKC, Rho A, MLCK and p-MLC protein expressions in contrast to the IND group (P<0.01, respectively) (Fig. 9D and E). By contrast, TA pretreatment efficiently redressed the abnormal changes in the above mentioned indexes in the IND-damaged GES-1 cells after transfected with CXCR4 siRNA (P<0.01, respectively) (Fig. 9D and E), which were also consistent with TA’ cytoprotection and promoting migration effects on the IND-impaired GES-1 cells (Fig. 5C). In brief, the CXCR4 knockdown results added to the testimony that CXCR4 siRNA and TA pretreatment could engender antagonistic effect on IND-impaired GES-1 cells. The present data suggested that CXCR4 was positively drawn into TA mediated cytoprotection and promoting migration.

TA administration implemented the gastroprotective effect on IND-induced gastric damage rats

Ultimately, TA' gastroprotection on the rat gastric mucosal lesion indcued by IND was assessed. As manifested in Fig. 10A, the GBF of ulcer margin in the IND group decreased to 39.06% in contrast to the control group (P<0.01). Preprocessing TA (1, 2 and 4 mg/kg) dramatically elevated the GBF of ulcer margin by 21.59%, 34.70% and 49.48% in contrast to the IND group (P<0.05 or P<0.01, respectively).

Gastric mucus, phospholipids and bicarbonate constitute the first protective screen of gastric mucosa, which effectively depresses the pernicious effects of invasive elements on gastric mucosa (He et al. 2020). Therefore, the quantity of gastric mucus adhered was an important indicator to evaluate the effect of drugs on gastric mucosa. As indicated in Fig. 10B, the experimental rats administrated IND by gavage caused a remarkable exhaustion of gastric mucus in contrast to the control group (P<0.01). TA preprocess (1, 2 and 4 mg/kg) effectively suppressed the exhaustion of gastric mucus, raised the amount of gastric mucus adhered by 70.50%, 125.64% and 184.87% in contrast to the IND group (P<0.01, respectively). As is known to all, the abnormal secretion of gastric acid secretion is an important factor leading to gastric mucosal layer lesion. Therefore, suppressing gastric acid secretion has become one of the important means to treat gastric mucosal injury (He et al. 2017b). In the current experiment, the total acidity and volume of the gastric effluents apparently elevated, the gastric pH markedly reduced in the IND group in contrast to the control group (P<0.01, respectively). Nevertheless, pretreatment with TA (1, 2 and 4 mg/kg) prominently dampened the total acidity and volume of the gastric effluents by 17.06%, 48.82%, 71.06% and 13.48%, 44.94%, 65.17%, raised the gastric pH by 17.77%, 42.13% and 68.53% in contrast to the IND group (P<0.05 or P<0.01, respectively) (Fig. 10D).

Modern studies found that the gastric mucosa had a "gastric mucosal defense barrier" system composed of defense factors: mucus bicarbonate barrier, mucosal barrier, epidermal growth factor, prostaglandin, etc, which coordinated with each other to resist the damage of attack elements to the gastric mucosa. However, when the above barrier was damaged or the secretion of protective factors was insufficient, the protective effect of gastric mucosa would be weakened, and gastric ulcer would occur under the irritant actions of attack elements such as pepsin and gastric acid (Yandrapu and Sarosiek 2015). In the current experiment, the ulcer area of IND group had topped out at 56.14 ±

4.39 mm^2; After pretreated with TA (1, 2 and 4 mg/kg), their ulcer areas fell to 29.27 ± 2.19, 17.59 ± 1.28, 7.67 ± 0.75 mm^2, and the ulcer inhibition rates were 47.72 ± 4.35, 68.49 ± 3.64, 86.25 ± 1.87 %, respectively in a dose-dependent manner, which significantly marked difference as in contrast to the IND group (P<0.01, respectively) (Fig.10 C and D). Gastric mucosal histomorphology by H&E dyeing further revealed that the gastric mucosal layers were clear, the epithelium was complete, the glands were arranged orderly, and there was no congestion and erosion in the control group; On the contrary, hyperemia, dilation and erosive bleeding of gastric mucosa, epithelial cell abscission, disordered arrangement of glands and inflammatory cell infiltration were observed, and its gastric mucosal damage scores of edema, hemorrhage, inflammatory cell infiltration and epithelial cell loss in the IND model reached 3.28 ± 0.56, 3.54 ± 0.58, 2.60 ± 0.47 and 2.65 ± 0.40, respectively, and there were dramatical difference in contrast to the control group (P<0.01, respectively). TA (1, 2 and 4 mg/kg) safeguarded gastric tissue against hemorrhagic lesion, obviously alleviated the gastric mucosal edema, hemorrhage, inflammatory cell infiltration and epithelial cell loss, its improvement ratios were 16.81%, 58.55%, 86.96%; 19.68%, 53.99%, 82.98%;21.15%, 70.61%, 88.53% and 42.31%, 70.83%, 87.82% in contrast to the IND group (P<0.05 or P < 0.01, respectively) (Fig. 10C and E).

TA suppressed miR-139 expression and activated the CXCR4/CXCL12/PLC/PKC/Rho A/MLC pathway in IND-induced gastric damage rats

After amply verifying gastroprotective effect of TA on the gastric impaired rats induced by IND, we next detected its underlying mechanism. Firstly, the gastric tissue miR-139 mRNA expression was analyzed by qRT-PCR. The miR-139 mRNA expression of IND-impaired gastric tissue in rats prominently raised in contrast to the control group (P<0.01); On the contrary, TA (1, 2 and 4 mg/kg) dramatically repressed miR-139 mRNA expression in contrast to the IND group (P<0.01, respectively) (Fig. 11A). The current experimental data were identical with the *in vitro* results.

Subsequently, we analyzed the associated protein expressions of the CXCR4/CXCL12/ PLC/PKC/Rho A/MLC pathway. the qRT-PCR and western blot data of rat gastric mucosa manifested that CXCR4 and CXCL12 mRNA and protein expressions noticeably cut down (P<0.01, respectively); TA pretreatment prominently elevated CXCR4 and CXCL12 mRNA and protein expressions by 22.06%, 99.89%, 178.86%, 75.98%, 152.89%, 256.14% and 22.57%, 95.66%,

214.95%, 34.77%, 75.23%, 214.90% (P<0.05 or P<0.01, respectively) (Fig. 11B and C). Moreover, their downstream p-PLC, p-PKC, Rho A, MLCK and p-MLC protein expressions were also measured, Fig. 11C manifested that p-PLC, p-PKC, Rho A, MLCK and p-MLC protein expressions of the IND group were markedly depressed in contrast to the control group (P<0.01, respectively). After pretreatment of TA, the abnormal protein expressions of p-PLC, p-PKC, Rho A, MLCK and p-MLC were obviously reversed in contrast to the IND group (P<0.05, P<0.01, respectively). The above-mentioned results demonstrated that miR-139 and its mediated downstream CXCR4/CXCL12/PLC/PKC/Rho A/MLC pathway were participated in TA-boosted the proliferation and migration of gastric epithelial cells, and then ameliorated the impaired gastric repair and healing process in the gastric impaired rats induced by IND, which was coincident with the data of *in vitro* experiments.

Discussion

Mugua is the dry and nearly mature fruit of *Chaenomeles speciosa* (Sweet) Nakai in Rosaceae plant, which is one kind of crop that has unique medicinal value and nutritional health care function, which also is a healthy food with lots of nutrients. In clinical practice, it is mainly used to treat dampness arthralgia and contracture, severe pain of waist and knee joint, vomiting and diarrhea in summer, muscle contracture pain, beriberi edema, etc (China Pharmacopoeia Committee 2020); At the same time, it is also a high-quality raw material for processing Mugua can, fruit pulp, wine, beverage and other food, skin care products and bath products. There is a folk saying of “apricot one benefit, pear two benefits and Mugua 100 benefits”, so Mugua is also known as “the fruit of 100 benefits” (He et al. 2020). In China, Tujia doctors and residents are used to soaking Mugua in corn wine to make Mugua wine, or picking immature Mugua to make appetizers (Mugua pickles, Mugua sauce and Mugua vinegar) and snacks (fruit juice, preserved fruits, preserves, etc.) to resist rheumatic diseases and gastrointestinal injuries that may be caused by the long rainy and humid mountain environment and the habit of eating spicy and pickled/smoked meat. Through the follow-up survey in recent 10 years, we did find that their probability of suffering from these two diseases is much lower than that in non-Mugua producing areas and people who do not eat Mugua (Wang et al. 2015). Inspired by these, we had successfully screened triterpenoids from the fruits of *Chaenomeles speciose*, and demonstrated that they have a good protective effect on IND-impaired rat gastric epithelial cells, GES-1 cells and ethanol and IND-impaired gastric lesion in mice and rats.

Triterpenoids from the fruits of *Chaenomeles speciose* were pentacyclic triterpenoids, which were separated into lupane-type triterpenoids (betulinic acid), oleanane-type triterpenoids (oleanolic acid, maslinic acid) and ursane-type triterpenoids (ursolic acid, 3-O-acetyl ursolic acid, 3-O-acetyl pomolic acid and TA) (Qin et al. 2016a; He et al. 2017a; Qin et al. 2015; Qin et al. 2016b; He et al. 2017b; Shi et al. 2016; Zhang et al. 2020; He et al. 2019). In order to compare the differences of their gastric protective effects and further explore its possible mechanism, we implemented the present study. In the study, our results manifested that TA was the most gastroprotective component of the pentacyclic triterpenoids (oleanolic acid, maslinic acid, betulinic acid, ursolic acid, 3-O-acetyl ursolic acid, 3-O-acetyl pomolic acid and TA) against IND-damaged GES-1 cells. Further studies confirmed that TA had protective effect on gastric lesion, which was associated with advancing IND-impaired GES-1 cell migration and proliferation, repressing apoptosis, meliorating IND-impaired rat GBF, ulcer area and inhibition rate, elevating the quantity of adherent gastric mucus, weakening the total acidity and volume of the gastric effluents, raising the gastric pH, mitigating submucosal edema, epithelial cell loss, gastric mucosal bleeding and suppressing inflammatory cell infiltration, upregulating mitochondrial viability, CXCR4 and CXCL12 mRNA and protein expressions, p-PLC, p-PKC, Rho A, MLCK and p-MLC protein expressions. Our current study manifested that TA's gastroprotective effect was closely correlated with suppressing miR-139 expression, activating activated CXCR4/CXCL12/PLC/PKC/Rho A/MLC pathway, which in turn promoted the migration and proliferation of gastric epithelial cells, and ameliorated the impaired gastric repair and healing.

Recently, miR-139 has been widely investigated in many human diseases, for example, osteoarthritis, bronchial asthma, myocardial injury, breast cancer and so on (Cheng et al. 2021). Zhang and his colleagues (Zhang et al. 2018) discovered that the expressions of miR-139 in breast cancer cell lines (MDA-MB-231, BT-474, MCF-7, SKBR3) and patient's breast cancer tissues were downregulated. Overexpression of miR-139 prominently repressed CXCR4 and CXCL12 expressions in MDA-MB-231 cells and suppressed cell metastasis *in vivo*, and confirmed that miR-139 restrained the CXCR4/CXCL12 signal axis to push down the metastasis of breast cancer. Furthermore, Baskara-Yhuellou and Tost (Baskara-Yhuellou and Tost 2020) also verified that the overexpression of miR-139 could retard the proliferation of bronchial smooth muscle cells, accelerate apoptosis, and ameliorate airway remodeling and hyperresponsiveness in asthma.

Interestingly, we first discovered that the mRNA expression of miR-139 was evidently raised, the mRNA and protein expressions of CXCR4 and CXCL12 were obviously depleted of the gastric ulcer patients, but the aforementioned expressions was effectively reversed with the gastric mucosa healing.[24] The miR-139 mRNA expressions in the IND-impaired GES-1 cells and rat gastric tissues manifested noticeably the increasing tendency in contrast to the GES-1 cells and rats, and preprocessing TA markedly repressed its expression in our research. Furthermore, the miR-139 overexpression attributed to miR-139 mimic transfection further exacerbated the cell damage induced by IND, which was related to cell proliferation and migration suppressions, mitochondrial viability depression and apoptosis elevation. In contract, the miR-139 knocked down by transfecting with miR-139 inhibitor or preprocessing TA used alone or combined using miR-139 inhibitor could notably accelerate cell proliferation and migration, hoist mitochondrial viability and restrain apoptosis. After preprocessing TA, the changes of gastric tissue miR-139 in the IND-impaired rats were also resemble to it.

It is generally known that miRs are participated in bioprocesses such as growth and development, differentiation, signal transduction, proliferation, migration and apoptosis, which play a leading role in a variety of pathophysiological processes, including trauma repair, tumors, by regulating its target genes (Cui et al. 2017). Therefore, it was necessary to further study the target genes regulated by miR-139 in our experiment. Therefore, we forecasted and verified it by using bioinformatics forecast and luciferase reporter gene analysis in the current study, the results demonstrated that miR-139 might directly combine to the 3'-UTR region of CXCR4 mRNA, and for this reason, CXCR4 might be credited as a target gene of miR-139. Chemokine receptor CXCR4 is a specific receptor for CXCL12, which involved in modulating the biological functions of proliferation, differentiation, migration, chemotaxis and strengthening angiogenesis, wound reepithelialization (Smith et al. 2005; Chen et al. 2021). Guo and his colleagues (Guo et al. 2015) indicated that the CXCL12 expression levels at the wound edges were dramatically elevated after injury, and CXCR4 expression were also substantially promoted in proliferating epithelial cells.

In addition, obstructing the CXCR4 and CXCL12 leaded to a remarkable repression in epidermal cell migration *in vitro* and slowed wound healing *in vivo*. After gastric mucosal injury, CXCR4 and its ligand CXCL12 constituted the chemokine-chemokine receptor axis in epithelial cell homing, and the activation of CXCR4 might play a major role in migrating pre-existing or

externally transplanted epithelial cells to the impaired site, and then repairing damaged gastric tissue and promoting wound healing. Moreover, *in vitro* chemotaxis experiments demonstrated that epithelial cells overexpressing CXCR4 could promote the migration to CXCL12 (Chen et al. 2021; Guo et al. 2015; Rao et al. 2001; Wang et al. 2021). Therefore, CXCR4 and CXCL12 play a crucial role in the impaired gastric healing. In the present study, the CXCR4 and CXCL12 mRNA and protein expressions were obviously repressed in IND-impaired GES-1 cells and rat gastric tissues, and the negative or positive regulatory relationship between them and miR-139 was further demonstrated by miR-139 mimic or miR-139 inhibitor experiment in IND-impaired GES-1 cells.

Moreover, transfection with CXCR4 siRNA might obviously reduce GES-1 cell migration, proliferation, facilitated apoptosis and miR-139 expression. By contrast, the miR-139 knocked down by transfecting with miR-139 inhibitor or preprocessing TA used alone or combined using miR-139 mimic, miR-139 mimic inhibitor or CXCR4 siRNA transfection in the IND-impaired GES-1 cells significantly reversed the reduced CXCR4 and CXCL12 mRNA and protein expressions. Preprocessing TA markedly elevated the gastric tissue CXCR4 and CXCL12 mRNA and protein expressions in the gastric damage rats induced by IND. Based on the above statements, we extrapolated that miR-139 negatively adjusted its downstream CXCR4 target. These findings demonstrated that TA's gastroprotective effect on IND-impaired GES-1 and rats was closely interrelated with curbing miR-139 expression and activating CXCR4/CXCL12 signal axis.

It has been well-documented that CXCR4/CXCL12/PLC/PKC/Rho A/MLC pathway plays a crucial role in repairing gastric mucosal lesion and find that CXCR4/CXCL12 signal axis facilitated the epithelial cell migration and the mucosal barrier repair are not an independent process, which needs the participation of a series of downstream signal pathways, such as PLC/PKC/Rho A/MLC pathway (Mi et al. 2021; Rodriguez et al. 2020; Shimada and Terano 1998). On the one hand, after CXCR4/CXCL12 activated, it might quickly activate G protein-coupled receptors on the surface of epithelial cells, trigger PLC/PKC signal cascade transmission through relevant adaptor molecules (such as Shc, PLC, etc.), activate Rho GTPase family members (for example, RhoA, Rac1 and Cdc42), induce the rapid phosphorylation of cytoskeleton molecule β-catenin, and then lead to the separation of E-cadherin/catenin compound from actin cytoskeleton and the instability of cell-cell adhesion connection, thus accelerate the phosphorylation of amino acid residues of tight junction proteins (such as claudin, occludin, JAM, ZO, cingulin, etc.), activate the integrin signal

transduction, boost the focal adhesion kinase phosphorylation, sabotage cell matrix adhesion, alter cytoskeleton, reinforces MLCK activity, accelerate MLC phosphorylation and then facilitate epithelial cell migration (Hwang et al. 2012; Rao et al. 2001; Akimoto et al. 2005; Amoozadeh et al. 2018; Carrasco-Pozo et al. 2016). When the epithelial cells migrated to the injured site, activated CXCR4/ CXCL12 could, on the other hand, stimulate epithelial cell repolarization, reconstitute cell-cell connection and cell matrix adhesion, advance epithelial cell proliferation and differentiation, reconstruct mucosal barrier, and then accelerate the impaired gastric healing through activating PLC/PKC/Rho A/MLC pathway (Rathinam et al. 2011; Aihara et al. 2018). All of these demonstrated that the impaired gastric healing was closely relevant to the activation of PLC/PKC/Rho A/MLC pathway mediated by CXCR4/CXCL12 signal axis. In our study, the obviously abated p-PLC, p-PKC, Rho A, MLCK and p-MLC protein expressions were detected in IND-impaired GES-1 cells and rat gastric tissues, and the aforementioned expression levels in the miR-139 mimic or CXCR4 siRNA-transfected GES-1 cells induced by IND were further worsen. While, transfection with miR-139 inhibitor might effectively keep these changes down.

Similarly, Whether TA used alone or in combined with miR-139 mimic or CXCR4 siRNA transfection in the IND-impaired GES-1 cells might successfully reverse the anomalous protein expressions of p-PLC, p-PKC, Rho A, MLCK and p-MLC; By contrast, TA used alone or in combined using miR-139 inhibitor transfection in the IND-impaired GES-1 cells further elevated the p-PLC, p-PKC, Rho A, MLCK and p-MLC protein expression levels. All of these outcomes were in keeping with the enhancements of proliferation, migration in IND-impaired GES-1 cells and the amelioration of GBF, gastric ulcer, gastric acid secretions, gastric damage scores and histopathological changes of gastric mucous tissue in IND-impaired rats. These data manifested that TA' gastroprotective effect on IND-impaired GES-1 cells and rats by activating CXCR4/ CXCL12/PLC/PKC/Rho A/MLC pathway.

Our results authenticated for the first time that TA owned protection characteristics against gastric mucosal injuries induced by IND *in vitro* and *vivo*, and its gastroprotective effects were tightly relevant to retarding miR-139 expression and activating CXCR4/CXCL12/PLC/PKC/ Rho A/MLC pathway, thereby boosting epithelial cell migration and proliferation, reconstructing mucosal barrier, and then accelerating the impaired gastric mucosa healing (Fig. 12). These data

furnished new slants for elucidating the potential mechanism of TA's gastroprotection and promised in serving as a candidate agent to treat gastric mucosal lesion.

Ethical Approval

The experimental procedures were carried out according to the guiding principle of the National Institutes of Health (Bethesda, USA). The experimental scheme was ratified by the Laboratory Animal Care and Use Committee of China Three Gorges University (CTGUEAC-2021-079).

Consent to Participate

The informed consent was obtained from all individual participants included in the study and agreed to participate. Before submitting revised manuscript, the authors of the manuscript have read the paper, and revised it under their helps for many times, at last, all authors agreed to submit the manuscript to Naunyn Schmiedebergs Arch Pharmacol.

Consent to Publish

This is an original research and has not been sent in any form for publication to other journals. The data presented in the MS are originally collected by the research activity at the laboratory. This is the first time to you. Before submitting revised manuscript, the authors of the manuscript have read the paper, and revised it under their helps for many times, at last, all authors agreed to submit and publish the manuscript to Naunyn Schmiedebergs Arch Pharmacol.

Authors Contributions

Junyu He, Adeline Ngeng Ngwa, Yuanyuan Zhang: Methodology, Experiment in vitro, Writing -original draft; Xiao Wang, Jie Li: Methodology, Experiment in vivo; Haibo He, Yumin He, Daoxiang Xu, Jihong Zhang: Conceptualization, Writing - original draft, Writing - review & editing, Funding acquisition, Supervision; Guofan Xu, Junzhi Wang, Kun Zou: revising, Supervision. All authors read and approved the manuscript and all data were generated in-house and that no paper mill was used.

Funding

This work was advocated by the Zhejiang Basic Public Welfare Research Program (LGF21H090002), the Zhejiang Medical and Health Science and Technology Plan Project

(2022497454), the Research Foundation of Yichang City Science and Technology Bureau (A21-2-044), the Open Foundation of Hubei Key Laboratory of Tumor Microenvironment and Immunotherapy (2018KZL01) and the Master Dissertation Foundation of China Three Gorges University (2020SSPY114).

Competing Interests

The authors declared that they had no conflicts of interests.

Availability of data and materials

NO.

References

Aihara E, Engevik KA. Montrose, MH (2017) Trefoil factor peptides and gastrointestinal function. Annu Rev Physiol 79: 357-380

Aihara E, Medina-Candelaria NM, Hanyu H, Matthis AL, Engevik KA, Gurniak CB, Witke W, Turner JR, Zhang T, Montrose MH (2018) Cell injury triggers actin polymerization to initiate epithelial restitution. J Cell Sci 131: jcs216317. doi: 10.1242/jcs.216317

Akimoto M, Hashimoto H, Shigemoto M, Maeda A, Yamashita K (2005) Effects of antisecretory agents on angiogenesis during healing of gastric ulcers. J Gastroenterol 40: 685-689

Amoozadeh Y, Anwer S, Dan QH, Venugopal S, Shi YX, Branchard E, Liedtke E, Ailenberg M, Rotstein OD, Kapus A, Szászi K (2018) Cell confluence regulates claudin-2 expression: possible role for ZO-1 and Rac. Am J Physiol Cell Physiol 314: C366-C378

Baskara-Yhuellou I, Tost J (2020) The impact of microRNAs on alterations of gene regulatory networks in allergic diseases. Adv Protein Chem Struct Biol 120: 237-312

Carrasco-Pozo C, Castillo RL, Beltrán C, Miranda A, Fuentes J, Gotteland M (2016) Molecular mechanisms of gastrointestinal protection by quercetin against indomethacin-induced damage: role of NF-κB and Nrf2. J Nutr Biochem 27: 289-298

Cheng CW, Liao WL, Chen PM, Yu JC, Shiau HP, Hsieh YH, Lee HJ, Cheng YC, Wu PE, Shen CY (2021) MiR-139 modulates cancer stem cell function of human breast cancer through targeting CXCR4. Cancers (Basel) 13: 2582. doi: 10.3390/cancers13112582

Chen HT, Li GC, Liu YQ, Ji SF, Li Y, Xiang JB, Zhou LX, Gao HH, Zhang WW, Sun XY, Fu XB, Li BH (2021) Pleiotropic roles of CXCR4 in wound repair and regeneration. Front Immunol 12: 668758. doi: 10.3389/fimmu.2021.668758

Chen L, Gao Y, Zhu LH, Song HJ, Zhao LL, Liu AH, Zhang GL, Shi GY (2018) Establishment and characterization of a GES-1 human gastric epithelial cell line stably expressing miR-23a. Oncol Lett 16: 977-983

Cherfils J, Zeghouf M (2013) Regulation of small GTPases by GEFs, GAPs, and GDIs. Physiol Rev 93: 269-309

China Pharmacopoeia Committee. Chinese Pharmacopoeia (I) (2020) China Medical Science and Technology Press: Beijing 62-63

Cho CJ, Mills JC (2019) Calcified, top secretion only: epithelial repair in gastric organoids requires calcium mobilization. Physiol 597: 2617-2618

Croitoru IC, CrăiŢoiu Ş, Petcu CM, Mihăilescu OA, Pascu RM, Bobic AG, Agop Forna D (2016) Clinical, imagistic and histopathological study of chronic apical periodontitis. Rom J Morphol Embryo 57: 719-728

Cui J, Zhou BY, Ross SA, Zempleni J (2017) Nutrition, microRNAs, and human health. Adv. Nutr 8: 105-112

Da B, Jani N, Gupta N, Jayaram P, Kankotia R, Yu CY, Dinis-Ribeiro M, Buxbaum J (2019) High-risk symptoms do not predict gastric cancer precursors. Helicobacter 24: e12548. doi: 10.1111/hel.12548

da Rosa RL, Nesello LÂN, Mariano LNB, Somensi LB, Campos A, Pinheiro AM, Costa S, Rial M, Tozzo M, Cechinel-Filho V, de Andrade SF, Da Silva LM (2018) Gastroprotective activity of the methanol extract from peels of *Plinia edulis* (Vell.) Sobral fruits and its isolated triterpenes: maslinic and ursolic acids. Naunyn Schmiedebergs Arch Pharmacol 391: 95-101

Dhiyaaldeen SM, Amin ZA, Darvish PH, Mustafa IF, Jamil MM, Rouhollahi E, Abdulla MA (2014) Protective effects of (1-(4-hydroxy-phenyl)-3-mtolyl-propenone chalcone in indomethacin induced gastric erosive damage in rats. BMC Vet Res 10: 961. doi: 10.1186/ s12917-014-0303-7

Engevik KA, Hanyu H, Matthis AL, Zhang TL, Frey MR, Oshima Y, Aihara E, Montrose MH (2019) Trefoil factor 2 activation of CXCR4 requires calcium mobilization to drive epithelial repair in gastric organoids. Physiol 597: 2673-2690

Gomes Rde C, Bonamin F, Darin DD, Seito LN, Di Stasi LC, Dokkedal AL, Vilegas W, Souza Brito AR, Hiruma-Lima CA (2009) Antioxidative action of methanolic extract and buthanolic fraction of Vochysia tucanorum Mart. in the gastroprotection. J Ethnopharmacol 121: 466-471

Guo R, Chai LL, Chen L, Chen WG, Ge LP, Li XG, Li HL, Li SR, Cao C (2015) Stromal cell-derived factor 1 (SDF-1) accelerated skin wound healing by promoting the migration and proliferation of epidermal stem cells. In Vitro Cell Dev Biol Anim 51: 578-585

He HB, Feng ML, Xu HY, Li XM, He YM, Qin HL, Zhang YF, Tang HB, Zou K (2020) Total triterpenoids from the fruits of *Chaenomeles speciosa* exerted gastroprotective activities on indomethacin-induced gastric damage via modulating microRNA-423-5p-mediated TFF/NAG-1 and apoptotic pathways. Food Funct 11: 662-679

He HB, Zhang YF, Li XM, Li XQ, Luo T, Zhang JH, Zhou Q, Cai SJ (2017a) Clinical study of Mugua triterpene tablets combined with omeprazole capsules in the treatment of upper gastrointestinal bleeding caused by non-steroidal anti-inflammatory drugs. Clin Chin Materia Medica 33: 209-212

He HB, Zhang YF, Li XM, Li XQ, Qin HL, Liu CX, Tang HB, Wang JZ, Zou K (2017b) Effect of triterpene from *Chaenomeles speciosa* (Sweet) Nakai on gastic acid secretion and gastric mucosal barrier function in indomethacin induced mice. Biotic Resources 39: 211-216

He HB, Li XM, He YM, Qin HL, Zhang YF, Xiong XJ, Wang JZ, Zou K (2019) Therapeutic effect of total triterpenoids of Chaenomeles speciosa combined with omeprazole on gastric ulcer induced by indomethacin in rats. Zhongguo Zhong Yao Za Zhi 44: 2338-2347

Hoffmann W (2005). Trefoil factors TFF (trefoil factor family) peptide-triggered signals promoting mucosal restitution. Cell Mol Life Sci 62: 2932-2938

Hwang S, Zimmerman NP, Agle KA, Turner JR, Kumar SN, Dwinell MB (2012) E-cadherin is critical for collective sheet migration and is regulated by the chemokine CXCL12 protein during restitution. J Biol Chem 287: 22227-222240

Ishikawa T, Donatini Rdos S, Diaz IE, Yoshida M, Bacchi EM, Kato ET (2008) Evaluation of gastroprotective activity of Plinia edulis (Vell.) Sobral (Myrtaceae) leaves in rats. J Ethnopharmacol 118: 527-529

Laine L, Weinstein WM (1988) Histology of alcoholic hemorrhagic "gastritis": a prospective evaluation. Gastroenterology 94: 1254-1262

Liu CY, Shi JX, Huang J, Shi XG, Zhang JJ, Wu JW (2018) Effects of Shenling-Baizhu-San on the tight junction and MLCK/MLC pathway in mice with ulcerative colitis. J Chin Med Mater 41: 2180-2184

Liu YW, Liu H, Wu J (2018) Progress in gastric mucosa protectant. Clin Med J 16: 8-12

Magierowski M, Magierowska K, Hubalewska-Mazgaj M, Sliwowski Z, Ginter G, Pajdo R, Chmura A, Kwiecien S, Brzozowski T (2017) Carbon monoxide released from its pharmacological donor, tricarbonyldichlororuthenium (II) dimer, accelerates the healing of pre-existing gastric ulcers. Br J Pharmacol 174: 3654-3668

Mi C, Li PJ, Ma FQ, Li WZ (2021) Effects of pantoprazole on RhoA/ROCK pathway and gastric mucosal microcirculation in rats with liver cirrhosis portal hypertension. China Pharmacist 24: 218-222

Nam JH, Jung HJ, Choi JW, Lee KT, Park HJ (2006) The anti-gastropathic and anti-rheumatic effect of niga-ichigoside F1 and 23-hydroxytormentic acid isolated from the unripe fruits of *Rubus coreanus* in a rat model. Biol Pharm Bull 29: 967-970

Namulema J, Nansunga M, Kato CD, Kalange M, Olaleye SB (2018) Thyroid hormones increase stomach goblet cell numbers and mucin expression during indomethacin induced ulcer healing in Wistar rats. Thyroid Res 11: 6. doi: 10.1186/s13044-018-0050-0

Niv Y, Banić M (2014) Gastric barrier function and toxic damage. Dig Dis 32: 235-242

O'Malley P (2003) Gastric ulcers and GERD: the new "plagues" of the 21st century update for the clinical. nurse. specialist. Clin Nurse Spec 17: 286-289

Pan HC, Peng ZL, Lin JD, Ren XS, Zhang GJ, Cui YK (2018) Forkhead box C1 boosts triple-negative breast cancer metastasis through activating the transcription of chemokine receptor-4. Cancer Sci 109: 3794-3804

Qin HL, Wang AL, Deng W, He HB, Yang XJ, Sun WJ, Wang JZ, Cheng F, Liu F (2015) Study of protective effect of ethyl acetate extract from *Chaenomeles speciosa* on mice acute gastric ulcer. Pharm Clin Chin Materia Medica 31: 45-49

Qin HL, Zhang YF, He HB, Tang HB, Liu CX, Wang JZ, Yan WH, Luo HJ (2016a) Anti-apoptotic effect of triterpene from *Chaenomeles speciosa* (Sweet) Nakaion in indomethacin induced RGM-1 cells. Chin J Clin Pharmacol Ther 21: 1347-1353

Qin HL, Zhang YF, Tang HB, Lu QQ, Yan WH, He HB, Wang JZ (2016b) Effect of ethyl acetate extract from *Chaenomeles speciosa* (Sweet) Nakaion on the expression of miR-423-5p, TFF1 and p53 in acute gastric ulcer mice. Clin Chin Materia Medica 32: 80-82

Rao JN, Li L, Golovina VA, Platoshyn O, Strauch ED, Yuan JX, Wang JY (2001) Ca^{2+}-RhoA signaling pathway required for polyaminedependent intestinal epithelial cell migration. Am J Physiol Cell Physiol 280: 993-1007

Rathinam R, Berrier A, Alahari SK (2011) Role of Rho GTPases and their regulators in cancer progression. Front Biosci 17: 2561-2571

Rodríguez JA, Astudillo L, Schmeda-Hirschmann G (2003) Oleanolic acid promotes healing of acetic acid-induced chronic gastric lesions in rats. Pharmacoll Res 48: 291-294

Rodriguez R, Pertino MW, Arcos C, Reichert L, Echeverria J, Simirgiotis M, Borquez J, Cornejo A, Areche C, Sepulveda B (2020) Gastroprotective Effects and Untargeted Metabolomics Analysis of *Lycium Minutifolium J.* Remy (Solanaceae). Foods 9: 565. doi: 10.3390/foods9050565.

Shimada T, Terano A (1998) Chemokine expression in Helicobacter pylori-infected gastric mucosa. J Gastroenterol 33: 613-617

Shi MQ, Qin HL, Zhang YF, Liu Y, Deng W, Yang WY, Wang JZ, Lu XC (2016) Effect of total triterpene from *Chaenomeles speciosa* (Sweet) Nakaion on cytokines in LPS-stimulated RAW264.7 cells. Pharm Clin Chin Materia Medica 32: 76-80

Smith JM, Johanesen PA, Wendt MK, Binion DG, Dwinell MB (2005) CXCL12 activation of CXCR4 regulates mucosal host defense through stimulation of epithelial cell migration and promotion of intestinal barrier integrity. Am J Physiol Gastrointest Liver Physiol 288: G316-G326

Wang JZ, Wang AL, He HB, She XX, He YM, Li S, Liu LQ, Luo T, Huang NY, Luo HJ, Zou K (2019) Trametenolic acid B protects against cerebral ischemia and reperfusion injury through modulation of microRNA-10a and PI3K/Akt/mTOR signaling pathways. Biomed Pharmacother 112: 108692. doi: 10.1016/j.biopha.2019.108692

Wang JZ, Yan XM, Tian HY, Zou K, He HB, Hu F, Huang WF, Zhang P, Deng ZS (2015) Application of backward selection method based on Tujia medical trialistic theory in new drug research. Chin Tradi Herb Drugs 46: 2189-2192

Wang K, Zhu HZ, Yang L, Xu QW, Ren FC (2021) miR-139 promotes homing of bone marrow mesenchymal stem cells (BMSCs) to lung tissues of asthmatic rats to inhibit inflammatory response of Th2 cells by down-regulating Notch1/Hes1 pathway. Chin J Cell Mol Immunol 37: 97-104

Wang YP, Zhang Y, Yang JN, Li HR, Wang JJ, Geng WT (2021) *Lactobacillus plantarum* MA2 ameliorates methionine and choline-deficient diet induced non-alcoholic fatty liver disease in rats by improving the intestinal microecology and mucosal barrier. Foods 10: 3126. doi: 10.3390/foods10123126.

Yandrapu H, Sarosiek J (2015) Protective factors of the gastric and duodenal mucosa: an overview. Curr Gastroenterol Rep 17: 24. doi: 10.1007/s11894-015-0452-2

Zhang YY, Xu HY, He HB, Li XM, Feng ML, He YM, Jiang WJ, Wang JZ, Xu DX, Zou K (2020) Total triterpenes from the fruits of *Chaenomeles speciosa* (Sweet) Nakai protects against indomethacin-induced gastric mucosal injury: involvement of TFF1-mediated EGF/EGFR and apoptotic pathways. J Pharm Pharmacol 72: 409-423

Zhang ZH, Kan YZ, Su ZJ (2018) Molecular mechanism of MiR-139 inhibiting directional metastasis of breast cancer by down-regulating CXCR4-CXCL12 bio-axis. China Cancer 27: 61-67

Legends for figures

Fig. 1 Chemical structures of the pentacyclic triterpenoids (oleanolic acid, ursolic acid, betulinic acid, 3-O-acetyl ursolic acid, 3-O-acetyl pomolic acid, maslinic acid and TA) from the fruits of *Chaenomeles speciose* (Sweet) Nakai, their effects on the IND-damaged cell proliferation and suppressed LDH leakage. (A) Chemical structures of the pentacyclic triterpenoids. (B) Cell viability of oleanane-type triterpenoids. (C) Cell viability of lupane-type triterpenoids. (D) Cell viability of ursane-type triterpenoids. (E) LDH leakage of oleanane-type triterpenoids. (F) LDH leakage of lupane-type triterpenoids. (G) LDH leakage of ursane-type triterpenoids. The results were indicated as the means ± SD (n=5). $^{\#}P<0.05$, $^{\#\#}P<0.01$ in contrast to the control group; $^{*}P<0.05$, $^{**}P<0.01$ in contrast to the IND group.

Fig. 2 TA promoted IND-impaired GES-1 cell proliferation. (A) Cell proliferation of IND-impaired GES-1 cells in the preprocessing TA used alone or combined using the miR-139 mimics. (B) Cell proliferation of IND-impaired GES-1 cells in the preprocessing TA used alone or combined using the miR-139 inhibitor. The data were indicated as the mean ± SD (n=5). $^{\#}P<0.05$, $^{\#\#}P<0.01$ in contrast to the control group; $^{*}P<0.05$, $^{**}P<0.01$ in contrast to the IND group; $^{\dagger}P<0.05$, $^{\dagger\dagger}P<0.01$ in contrast to the mimic NC or inhibitor NC group.

Fig. 3 TA restrained IND-impaired GES-1 cell apoptosis. (A and B) Apoptotic cells by Hoechst-staining analysis. (C and D) Apoptotic cells. (E and F) Mitochondrial viability. The IND-impaired GES-1 cells were preprocessed TA used alone or combined using the miR-139 mimics and miR-139 inhibitor. Typical apoptotic cells were demonstrated by a green arrow marks. The results were indicated as the mean ± SD (n=5). $^{\#}P<0.05$, $^{\#\#}P<0.01$ in contrast to the control group; $^{*}P<0.05$, $^{**}P<0.01$ in contrast to the IND group; $^{\dagger}P<0.05$, $^{\dagger\dagger}P<0.01$ in contrast to the mimic NC or inhibitor NC group.

Fig. 4 TA boosted IND-impaired GES-1 cell migration. (A and B) Cell migration by wound healing assay. (C and D) Cell migration by Transwell assay. The IND-damaged GES-1 cells were preprocessed TA used alone or combined using the miR-139 mimics and miR-139 inhibitor. The results were indicated as the mean ± SD (n=5). $^{\#}P<0.05$, $^{\#\#}P<0.01$ in contrast to the control group; $^{*}P<0.05$, $^{**}P<0.01$ in contrast to the IND group; $^{\dagger}P<0.05$, $^{\dagger\dagger}P<0.01$ in contrast to the mimic NC or inhibitor NC group.

Fig. 5 TA facilitated IND-impaired GES-1 cell migration via downregulating miR-139 and activating CXCR4/CXCL12/PLC/PKC/Rho A/MLC pathway. (A) miR-139 mRNA expression. (B) CXCR4 and CXCL12 mRNA expressions. (C) Related protein expressions of CXCR4/ CXCL12/PLC/PKC/Rho A/MLC pathway. The IND-impaired GES-1 cells were preprocessed TA used alone or combined using the miR-139 mimics. The results were indicated as the mean ± SD (n=5). $^{\#}P<0.05$, $^{\#\#}P<0.01$ in contrast to the control group; $^{*}P<0.05$, $^{**}P<0.01$ in contrast to the IND group; $^{\dagger}P<0.05$, $^{\dagger\dagger}P<0.01$ in contrast to the mimic NC group.

Fig. 6 miR-139 knockdown reinforced the accelerating effect of TA on CXCR4/CXCL12/ PLC/PKC/Rho A/MLC pathway. (A) miR-139 mRNA expression. (B) CXCR4 and CXCL12 mRNA expressions. (C) Related protein expressions of CXCR4/CXCL12/PLC/PKC/Rho A/MLC pathway. The IND-impaired GES-1 cells were preprocessed TA used alone or combined using the miR-139 inhibitor. The results were indicated as the mean ± SD (n=5). $^{\#}P<0.05$, $^{\#\#}P<0.01$ in contrast to the control group; $^{*}P<0.05$, $^{**}P<0.01$ in contrast to the IND group; $^{\dagger}P<0.05$, $^{\dagger\dagger}P<0.01$ in contrast to the inhibitor NC group.

Fig. 7 CXCR4 was the direct target of miR-139. (A) miR-139 binding site in the 3′-UTR of CXCR4 forecasted by bioinformatics assay. (B) The luciferase activity analysis. (C) CXCR4 mRNA expression. (D and E) CXCR4 protein expression. The GES-1 cells were preprocessed TA used alone or combined using the miR-139 mimics and miR-139 inhibitor. The results were indicated as the mean ± SD (n=5). $^{\#}P<0.05$, $^{\#\#}P<0.01$ in contrast to the mimic NC group; $^{*}P<0.05$, $^{**}P<0.01$ in contrast to the inhibitor NC group; $^{\dagger}P<0.05$, $^{\dagger\dagger}P<0.01$ in contrast to the control group; $^{\triangle}P<0.05$, $^{\triangle\triangle}P<0.01$ in contrast to the TA group.

Fig. 8 CXCR4 knockdown attenuated the cytoprotection and migration of TA against IND-impaired GES-1 cells. (A) CXCR4 mRNA expression level. (B) CXCR4 protein expression level. (C) Cell viability analyzed by MTT method. (D) Cell proliferation detected by colony formation analysis. (E) Mitochondrial viability analyzed by flow cytometry. (F) Apoptotic cells detected by Hoechst-staining. (G) Apoptotic cells analyzed by flow cytometry. The GES-1 and IND-impaired GES-1 cells were transfected with CXCR4 siRNA. The results were indicated as the mean ± SD (n=5). $^{\#}P<0.05$, $^{\#\#}P<0.01$ in contrast to the control group; $^{*}P<0.05$, $^{**}P<0.01$ in contrast to the IND group; $^{\dagger}P<0.05$, $^{\dagger\dagger}P<0.01$ in contrast to the CXCR4 siRNA group.

Fig. 9 CXCR4 knockdown suppressed the migration and CXCR4/CXCL12/PLC/PKC/Rho A/MLC pathway activation of TA on IND-impaired GES-1 cells. (A) Cell migration by wound healing assay. (B) miR-139 mRNA expression. (C) Cell migration by Transwell assay. (D) CXCR4 and CXCL12 mRNA expressions. (E) Related protein expressions of CXCR4/ CXCL12/PLC/PKC/Rho A/MLC pathway. The GES-1 and IND-impaired GES-1 cells were transfected with CXCR4 siRNA. The results were indicated as the mean ± SD (n=5). $^{\#}P<0.05$, $^{\#\#}P<0.01$ in contrast to the control group; $^{*}P<0.05$, $^{**}P<0.01$ in contrast to the IND group; $^{\dagger}P<0.05$, $^{\dagger\dagger}P<0.01$ in contrast to the CXCR4 siRNA group.

Fig. 10 TA administration implemented gastroprotection on the gastric impaired rats induced by IND. (A) GBF. (B) Gastric mucosa mucus level. (C) Representative gastric photos of macro-lay and micro-lay. (D) Gastric ulcer and acid secretions. (E) Gastric lesion scores. Ulcer and damages were manifested by green arrow marks. The results were indicated as the mean ± SD (n=10). $^{\#}P<0.05$, $^{\#\#}P<0.01$ in contrast to the control group; $^{*}P<0.05$, $^{**}P<0.01$ in contrast to the IND group. Original magnification ×200 and ×400.

Fig. 11 TA restrained miR-139 expression and activated CXCR4/CXCL12/PLC/PKC/Rho A/MLC pathway in the gastric damage rats induced by IND. (A) miR-139 mRNA expression. (B) CXCR4 and CXCL12 mRNA expressions. (C) Related protein expressions of CXCR4/CXCL12/PLC/PKC/Rho A/MLC pathway. The results were indicated as the means ± SD (n=5). $^{\#}P<0.05$, $^{\#\#}P<0.01$ in contrast to the control group; $^{*}P<0.05$, $^{**}P<0.01$ in contrast to the IND group.

Fig. 12 Prospective molecular mechanism of TA-exerted gastroprotect on the gastric lesion induced by IND.

Table 1. Primer sequences used in qRT-PCR

Genes	**Forward primer (5′-3′)**	**Reverse primer (5′-3′)**
hsa-miR-139	ACACTCCAGCTGGGTCTACAGTGCACGTGTC	TGGTGTCGTGGAGTCG
hCXCR4	TGGCCTTATCCTGCCTGGTAT	GGAGTCGATGCTGATCCCAAT
hCXCL12	CTCAACACTCCAAACTGTGCCC	CTCCAGGTACTCCTGAATCCAC
rno-miR-139	ACACTCCAGCTGGGTCTACAGTGCAC	TGGTGTCGTGGAGTCG
rCXCR4	CGAGCATTGCCATGGAAATA	CGGAAGCAGGGTTCCTTGT
rCXCL12	AGCCAACGTCAAACATCTGAAA	CGGGTCAATGCACACTTGTC
U6	GATCCCTCCAAAATCAAGTGG	GGCAGAGATGATGACCCTTTT
GAPDH	GAAGGTGAAGGTCGGAGTC	GAAGATGGTGATGGGATTTG

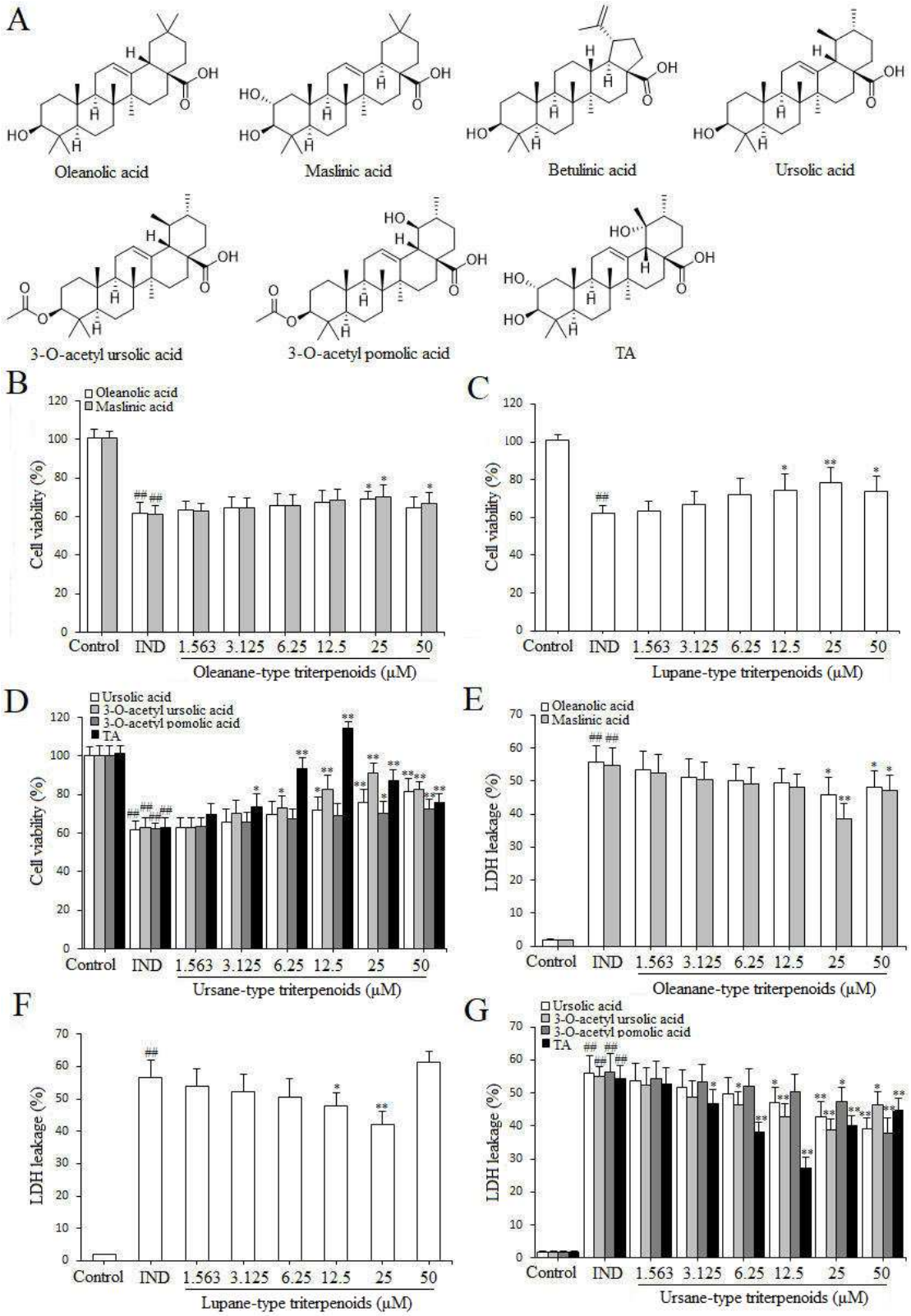
A
Oleanolic acid
Maslinic acid
Betulinic acid
Ursolic acid
3-O-acetyl ursolic acid
3-O-acetyl pomolic acid
TA
B
Oleanolic acid
Maslinic acid
Cell viability (%)
Control
IND
1.563
3.125
6.25
12.5
25
50
Oleanane-type triterpenoids (μM)
C
Cell viability (%)
Lupane-type triterpenoids (μM)
D
Ursolic acid
3-O-acetyl ursolic acid
3-O-acetyl pomolic acid
TA
Cell viability (%)
Ursane-type triterpenoids (μM)
E
Oleanolic acid
Maslinic acid
LDH leakage (%)
Oleanane-type triterpenoids (μM)
F
LDH leakage (%)
Lupane-type triterpenoids (μM)
G
Ursolic acid
3-O-acetyl ursolic acid
3-O-acetyl pomolic acid
TA
LDH leakage (%)
Ursane-type triterpenoids (μM)

Fig. 1

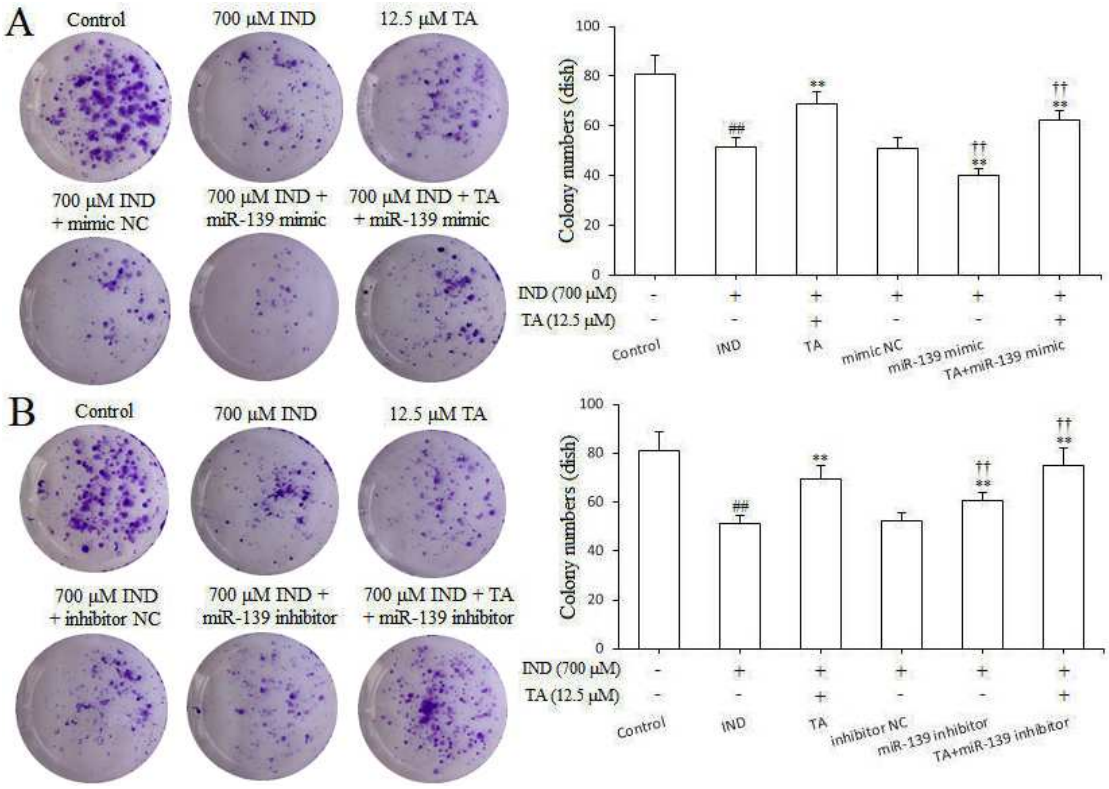
A
Control
700 μM IND
12.5 μM TA
700 μM IND + mimic NC
700 μM IND + miR-139 mimic
700 μM IND + TA + miR-139 mimic
Colony numbers (dish)
IND (700 μM)
TA (12.5 μM)
Control
IND
TA
mimic NC
miR-139 mimic
TA+miR-139 mimic
B
Control
700 μM IND
12.5 μM TA
700 μM IND + inhibitor NC
700 μM IND + miR-139 inhibitor
700 μM IND + TA + miR-139 inhibitor
Colony numbers (dish)
IND (700 μM)
TA (12.5 μM)
Control
IND
TA
inhibitor NC
miR-139 inhibitor
TA+miR-139 inhibitor

Fig. 2

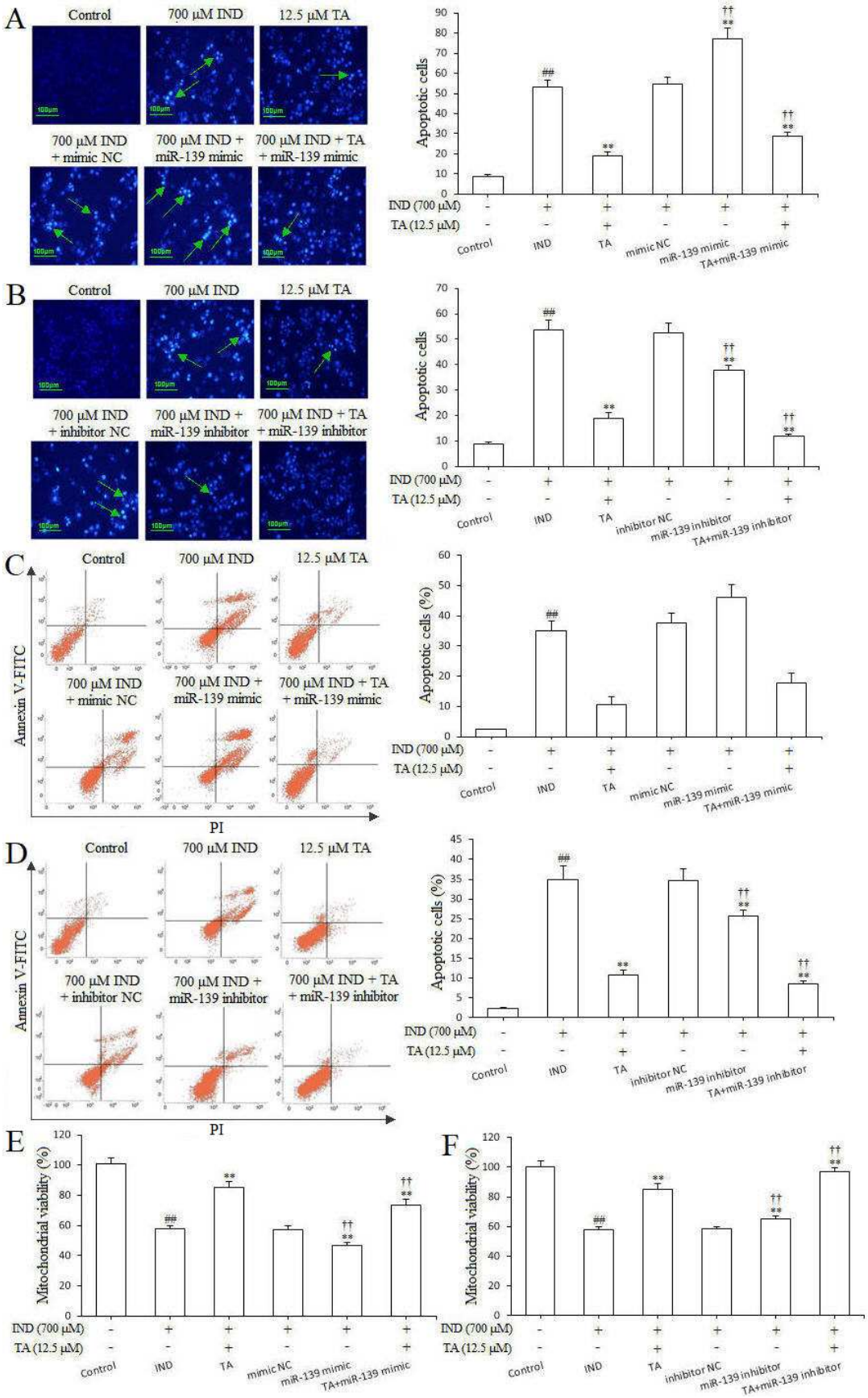
A
Control
700 μM IND
12.5 μM TA
700 μM IND + mimic NC
700 μM IND + miR-139 mimic
700 μM IND + TA + miR-139 mimic
Apoptotic cells
IND (700 μM)
TA (12.5 μM)
Control
IND
TA
mimic NC
miR-139 mimic
TA+miR-139 mimic
B
700 μM IND + inhibitor NC
700 μM IND + miR-139 inhibitor
700 μM IND + TA + miR-139 inhibitor
inhibitor NC
miR-139 inhibitor
TA+miR-139 inhibitor
C
Annexin V-FITC
PI
Apoptotic cells (%)
D
E
Mitochondrial viability (%)
F

Fig. 3

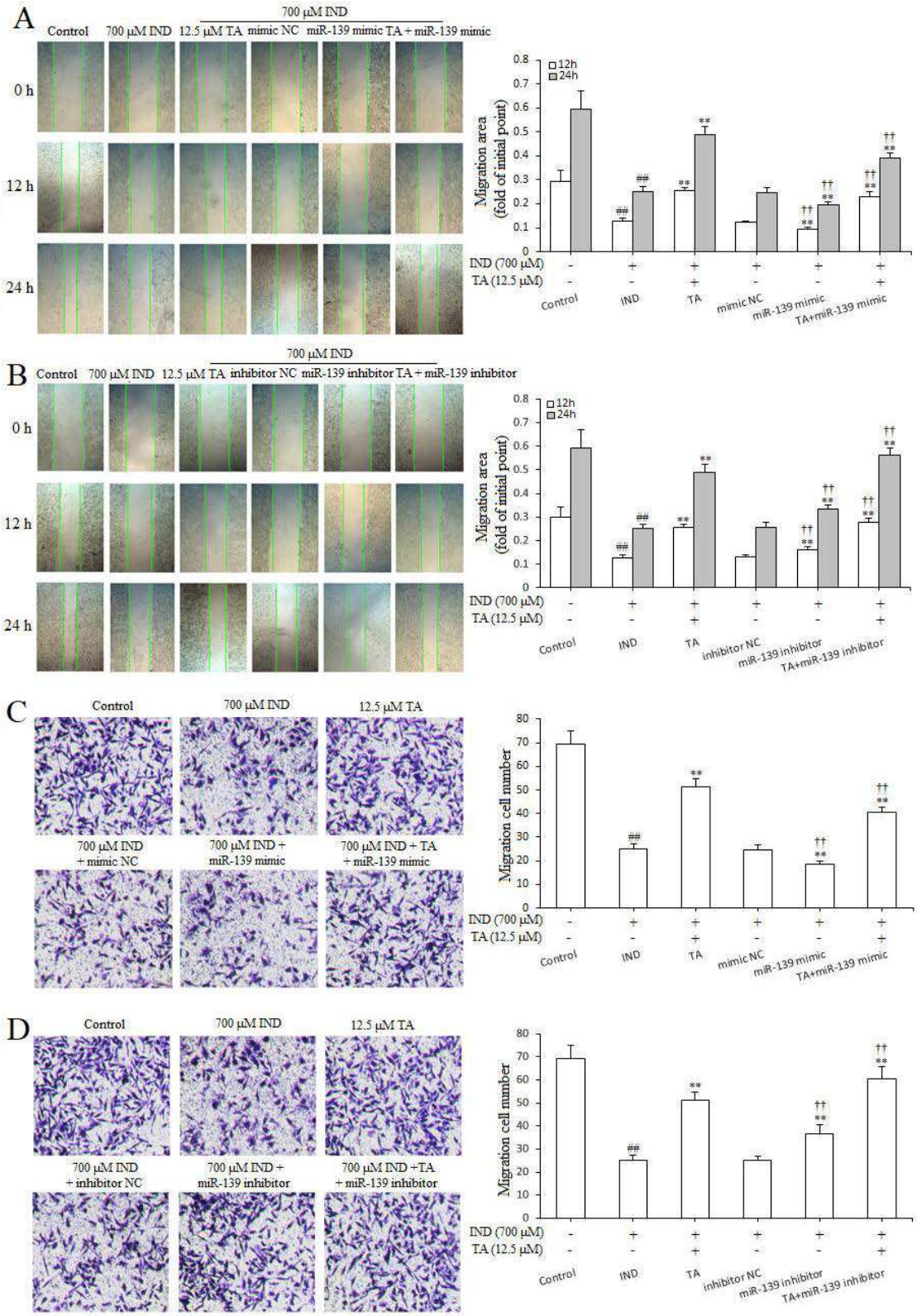
A
700 μM IND
Control
700 μM IND
12.5 μM TA
mimic NC
miR-139 mimic
TA + miR-139 mimic
0 h
12 h
24 h
12h
24h
Migration area (fold of initial point)
IND (700 μM)
TA (12.5 μM)
Control
IND
TA
mimic NC
miR-139 mimic
TA+miR-139 mimic
B
700 μM IND
Control
700 μM IND
12.5 μM TA
inhibitor NC
miR-139 inhibitor
TA + miR-139 inhibitor
0 h
12 h
24 h
12h
24h
Migration area (fold of initial point)
IND (700 μM)
TA (12.5 μM)
Control
IND
TA
inhibitor NC
miR-139 inhibitor
TA+miR-139 inhibitor
C
Control
700 μM IND
12.5 μM TA
700 μM IND + mimic NC
700 μM IND + miR-139 mimic
700 μM IND + TA + miR-139 mimic
Migration cell number
IND (700 μM)
TA (12.5 μM)
Control
IND
TA
mimic NC
miR-139 mimic
TA+miR-139 mimic
D
Control
700 μM IND
12.5 μM TA
700 μM IND + inhibitor NC
700 μM IND + miR-139 inhibitor
700 μM IND + TA + miR-139 inhibitor
Migration cell number
IND (700 μM)
TA (12.5 μM)
Control
IND
TA
inhibitor NC
miR-139 inhibitor
TA+miR-139 inhibitor

Fig. 4

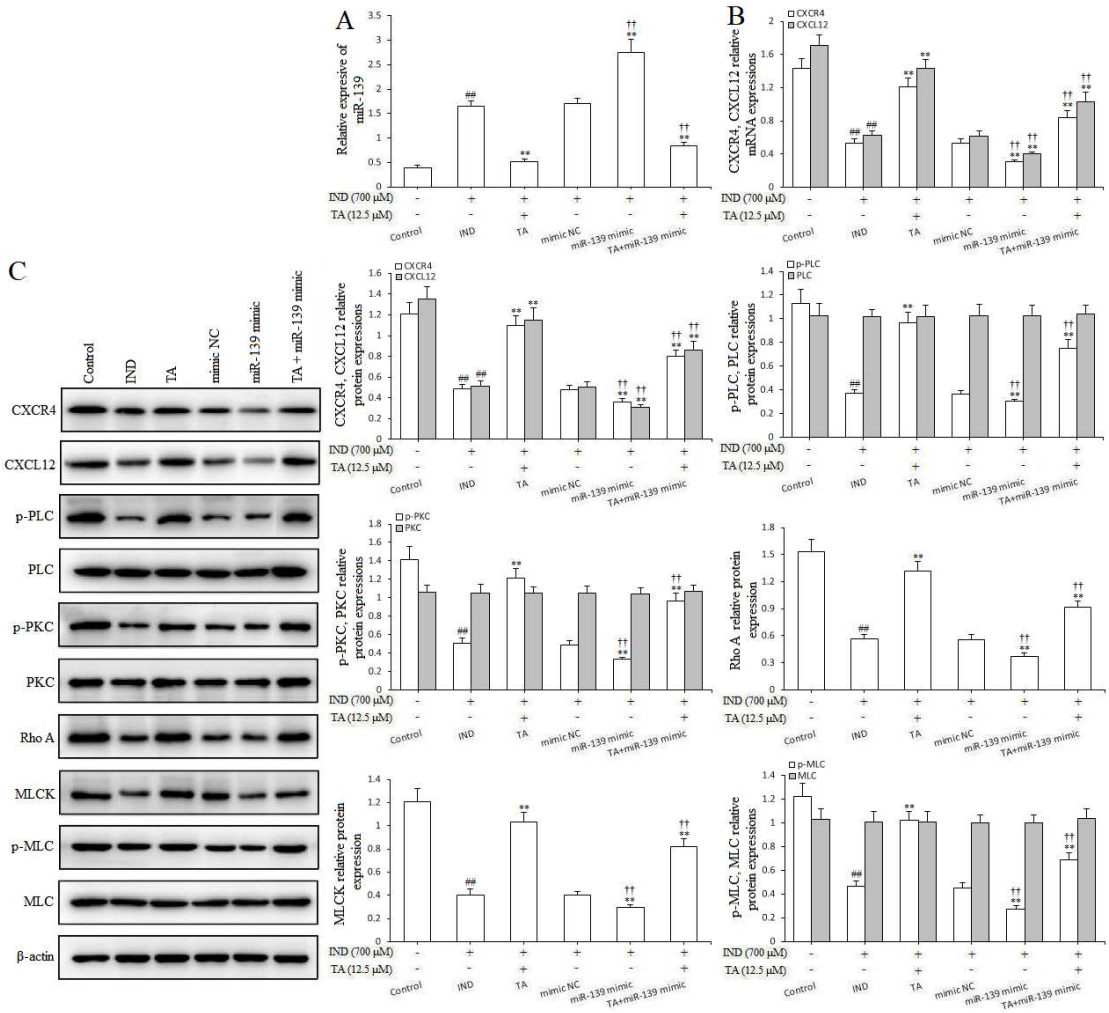
A
Relative expresive of miR-139
B
CXCR4
CXCL12
CXCR4, CXCL12 relative mRNA expressions
C
Control
IND
TA
mimic NC
miR-139 mimic
TA + miR-139 mimic
CXCR4
CXCL12
p-PLC
PLC
p-PKC
PKC
Rho A
MLCK
p-MLC
MLC
β-actin
CXCR4, CXCL12 relative protein expressions
p-PLC, PLC relative protein expressions
p-PKC, PKC relative protein expressions
Rho A relative protein expression
MLCK relative protein expression
p-MLC, MLC relative protein expressions
IND (700 μM)
TA (12.5 μM)
Control
IND
TA
mimic NC
miR-139 mimic
TA+miR-139 mimic

Fig. 5

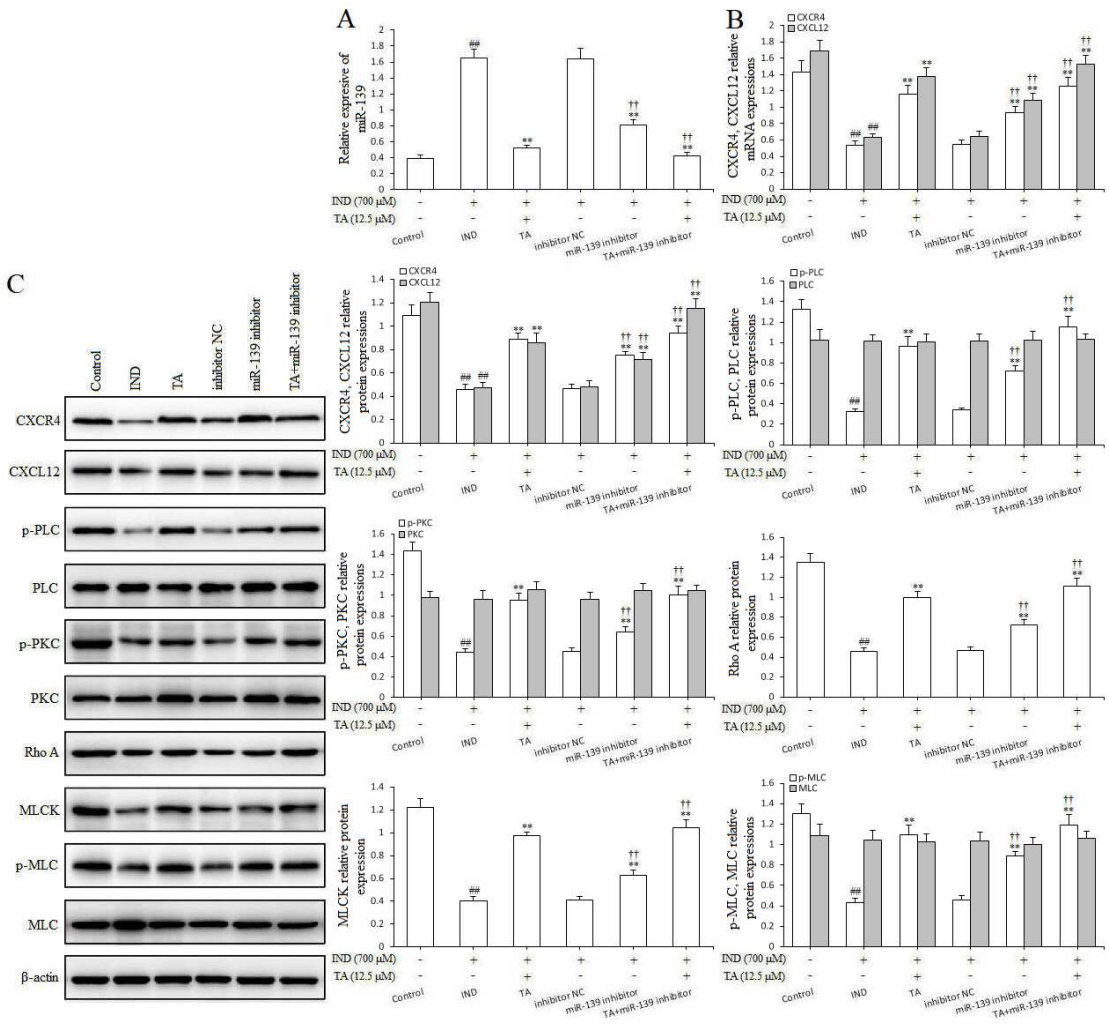
A
Relative expresive of miR-139
B
CXCR4
CXCL12
CXCR4, CXCL12 relative mRNA expressions
C
Control
IND
TA
inhibitor NC
miR-139 inhibitor
TA+miR-139 inhibitor
CXCR4
CXCL12
p-PLC
PLC
p-PKC
PKC
Rho A
MLCK
p-MLC
MLC
β-actin
CXCR4, CXCL12 relative protein expressions
p-PLC, PLC relative protein expressions
p-PKC, PKC relative protein expressions
Rho A relative protein expression
MLCK relative protein expression
p-MLC, MLC relative protein expressions
IND (700 μM)
TA (12.5 μM)

Fig. 6

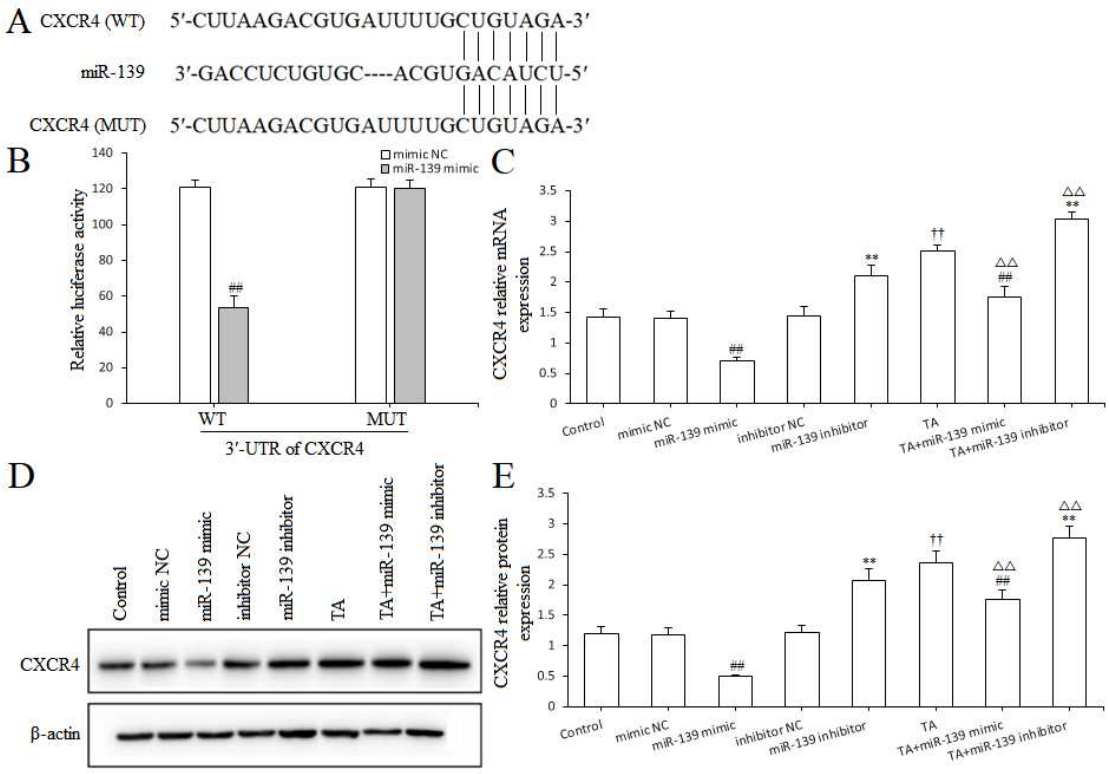
A
CXCR4 (WT) 5′-CUUAAGACGUGAUUUUGCUGUAGA-3′
miR-139 3′-GACCUCUGUGC----ACGUGACAUCU-5′
CXCR4 (MUT) 5′-CUUAAGACGUGAUUUUGCUGUAGA-3′
B
mimic NC
miR-139 mimic
Relative luciferase activity
WT
MUT
3′-UTR of CXCR4
C
CXCR4 relative mRNA expression
Control
mimic NC
miR-139 mimic
inhibitor NC
miR-139 inhibitor
TA
TA+miR-139 mimic
TA+miR-139 inhibitor
D
Control
mimic NC
miR-139 mimic
inhibitor NC
miR-139 inhibitor
TA
TA+miR-139 mimic
TA+miR-139 inhibitor
CXCR4
β-actin
E
CXCR4 relative protein expression

Fig. 7

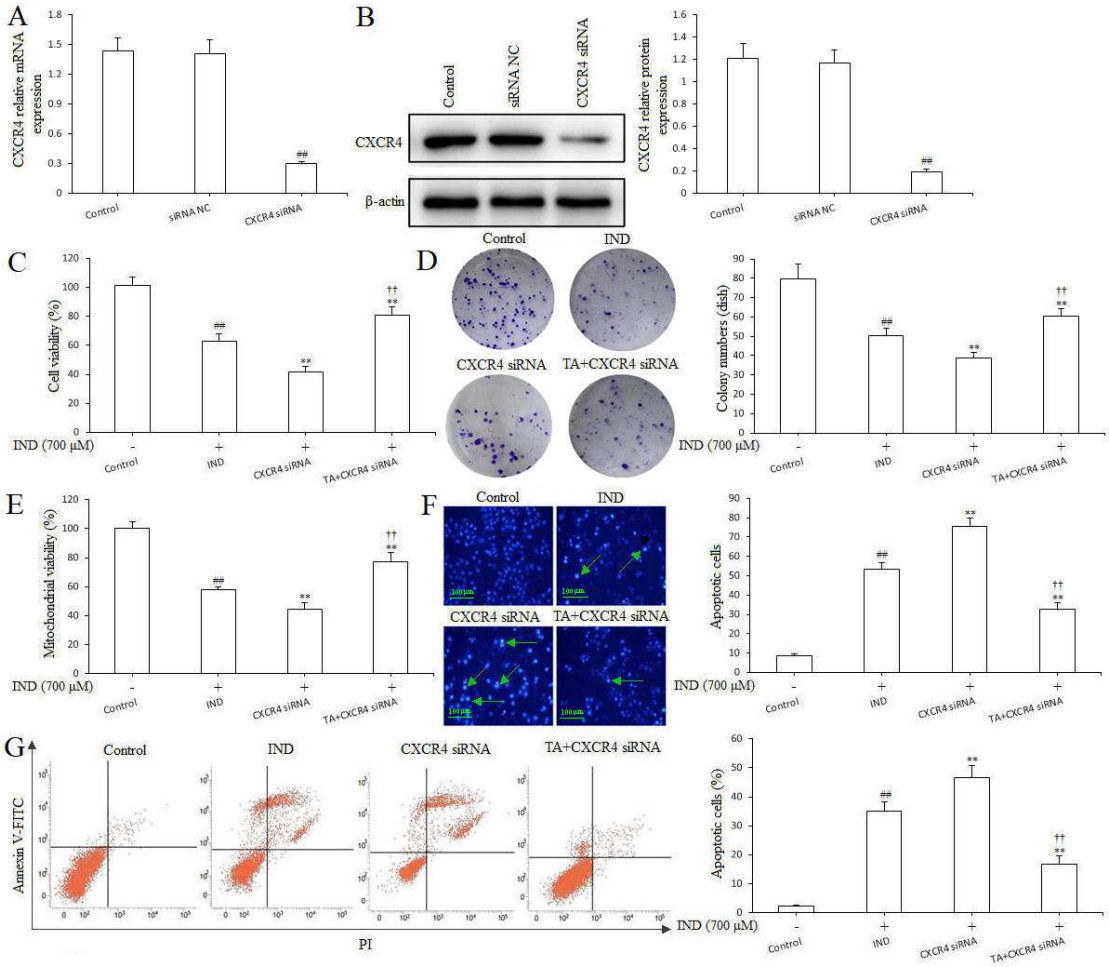
A
CXCR4 relative mRNA expression
Control
siRNA NC
CXCR4 siRNA
B
Control
siRNA NC
CXCR4 siRNA
CXCR4
β-actin
CXCR4 relative protein expression
C
Cell viability (%)
IND (700 μM)
Control
IND
CXCR4 siRNA
TA+CXCR4 siRNA
D
Control
IND
CXCR4 siRNA
TA+CXCR4 siRNA
Colony numbers (dish)
E
Mitochondrial viability (%)
F
Apoptotic cells
G
Annexin V-FITC
PI
Apoptotic cells (%)

Fig. 8

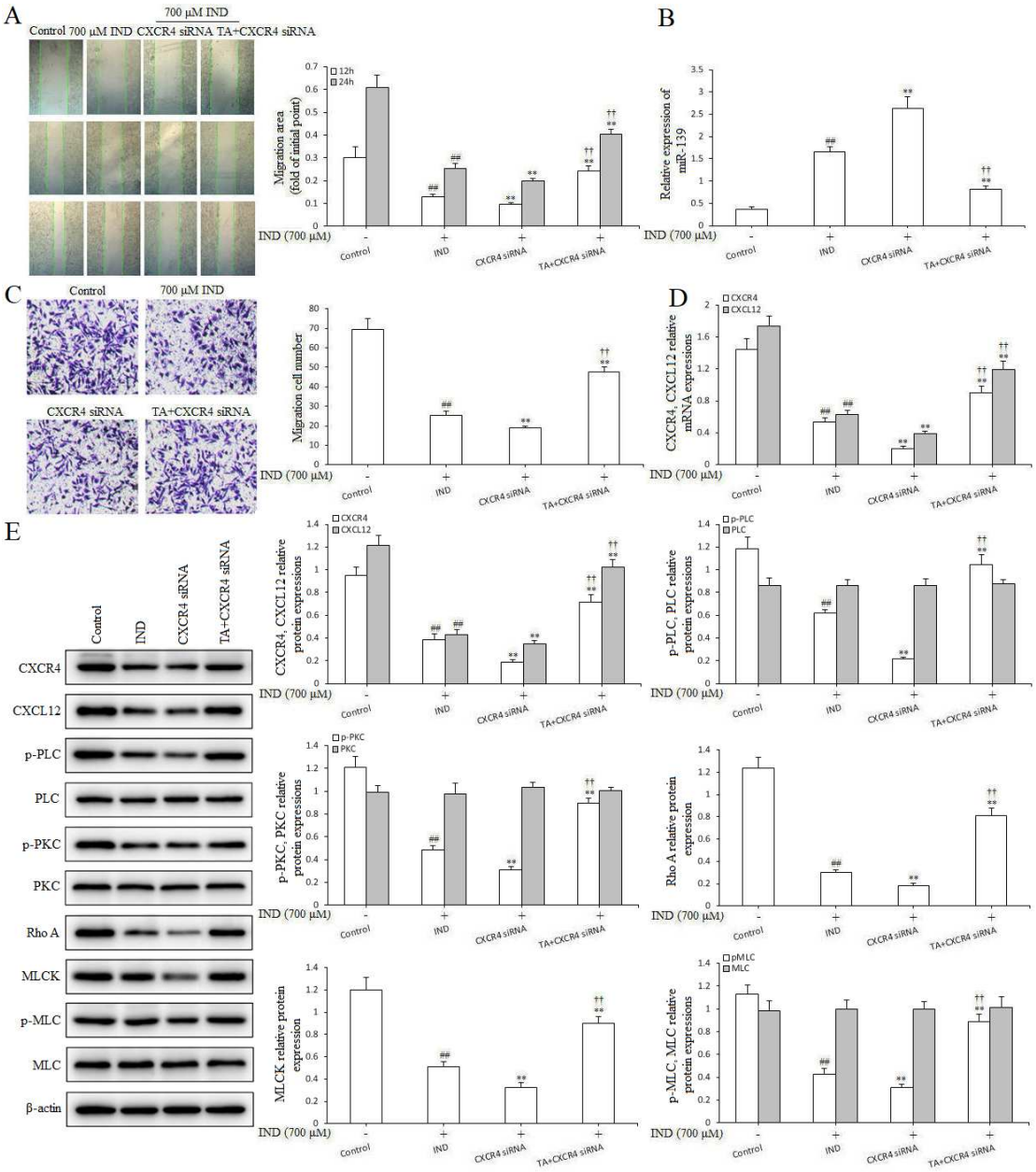
A
700 μM IND
Control 700 μM IND CXCR4 siRNA TA+CXCR4 siRNA
12h
24h
Migration area (fold of initial point)
IND (700 μM)
Control
IND
CXCR4 siRNA
TA+CXCR4 siRNA
B
Relative expression of miR-139
C
Control
700 μM IND
CXCR4 siRNA
TA+CXCR4 siRNA
Migration cell number
D
CXCR4
CXCL12
CXCR4, CXCL12 relative mRNA expressions
E
Control
IND
CXCR4 siRNA
TA+CXCR4 siRNA
CXCR4
CXCL12
p-PLC
PLC
p-PKC
PKC
Rho A
MLCK
p-MLC
MLC
β-actin
CXCR4, CXCL12 relative protein expressions
p-PLC, PLC relative protein expressions
p-PKC, PKC relative protein expressions
Rho A relative protein expression
MLCK relative protein expression
p-MLC, MLC relative protein expressions
pMLC

Fig. 9

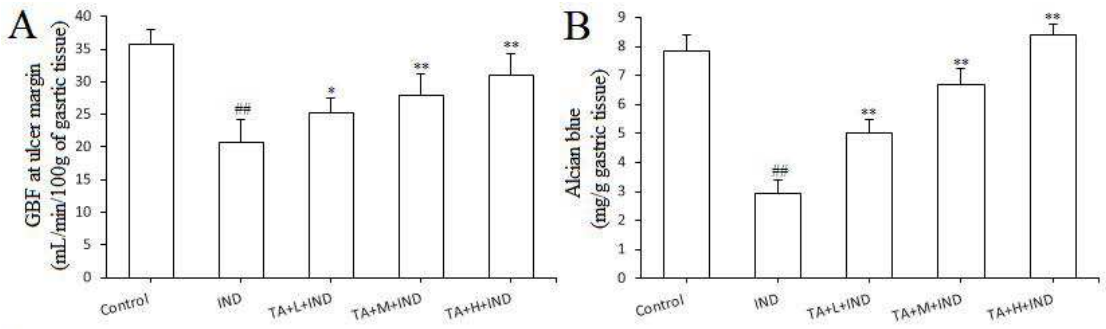

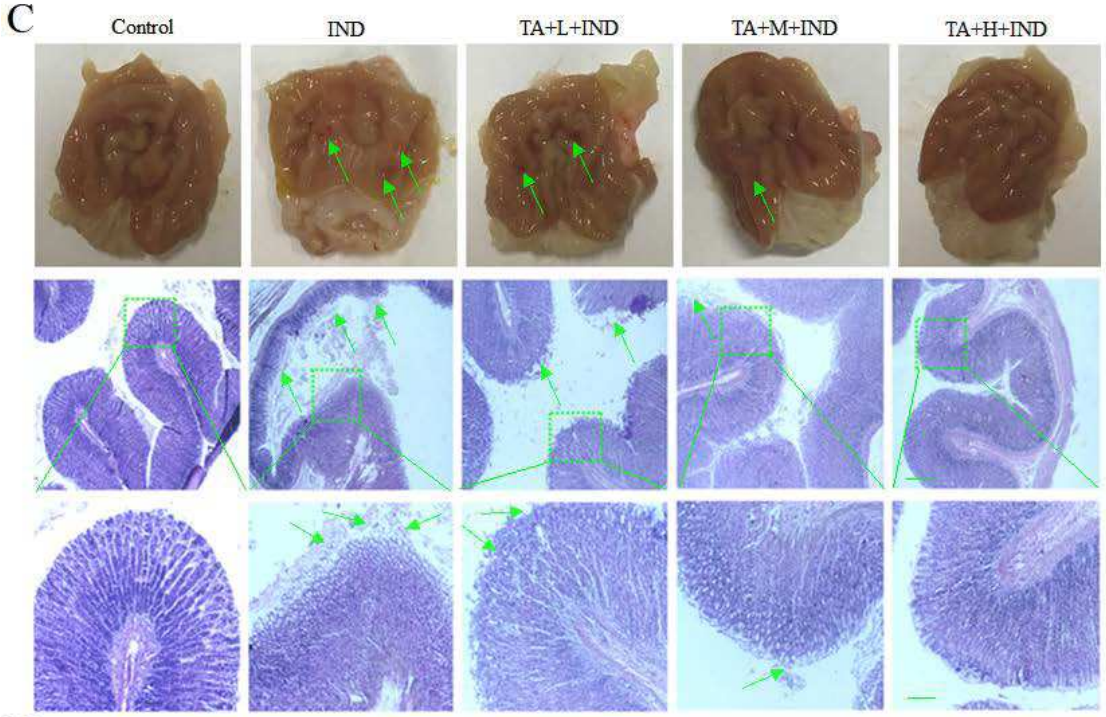

D

Experimental group	Ulcer area (mm^2)	Ulcer inhibitor (%)	Gastric juice volume (mL)	pH(Units)	$[H^+]$ (mEq/L4h)
Control	0.00 ± 0.00	----	0.18 ± 0.02	3.49 ± 0.28	1.76 ± 0.14
IND	56.14 ± 4.39 ##	0.00 ± 0.00	0.89 ± 0.08 ##	1.97 ± 0.19 ##	8.50 ± 0.81 ##
TA-L+IND	29.27 ± 2.19 **	47.72 ± 4.35 **	0.77 ± 0.07 *	2.32 ± 0.20 *	7.05 ± 0.72 *
TA-M-IND	17.59 ± 1.28 **	68.49 ± 3.64 **	0.49 ± 0.06 **	2.80 ± 0.23 **	4.35 ± 0.43 **
TA-H+IND	7.67 ± 0.75 **	86.25 ± 1.87 **	0.31 ± 0.03 **	3.32 ± 0.26 **	2.46 ± 0.22 **

E

Experimental group	Hemorrhage score	Edema score	Epithelial cell loss score	Inflammatory cell score	Total score
Control	0.00 ± 0.00	0.00 ± 0.00	0.11 ± 0.02	0.00 ± 0.00	0.11 ± 0.02
IND	3.76 ± 0.38 ##	3.45 ± 0.34 ##	3.12 ± 0.27 ##	2.79 ± 0.35 ##	13.13 ± 0.87 ##
TA-L+IND	3.02 ± 0.40 *	2.87 ± 0.26 *	1.80 ± 0.12 **	2.20 ± 0.26 *	9.90 ± 0.63 **
TA-M-IND	1.73 ± 0.15 **	1.43 ± 0.17 **	0.91 ± 0.07 **	0.82 ± 0.08 **	4.89 ± 0.21 **
TA-H+IND	0.64 ± 0.06 **	0.45 ± 0.04 **	0.38 ± 0.03 **	0.32 ± 0.03 **	1.79 ± 0.05 **

Fig. 10

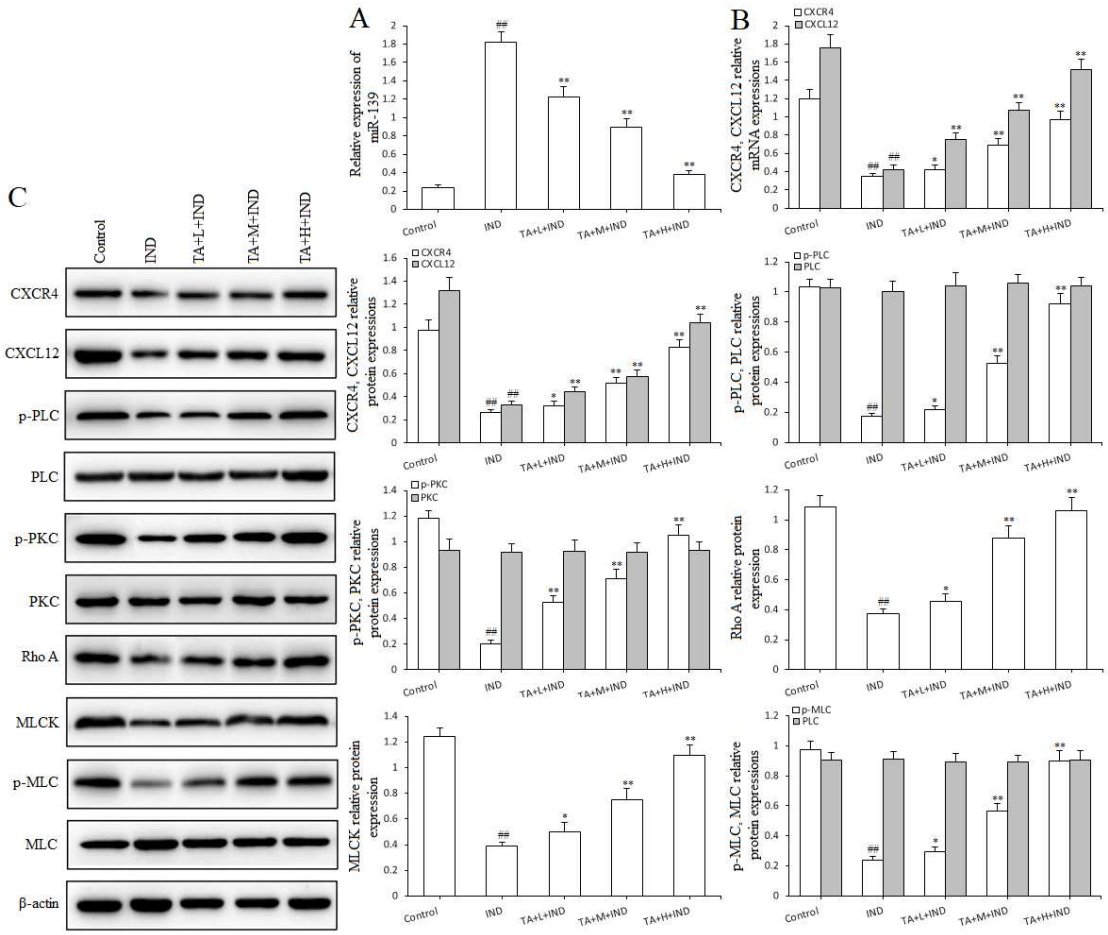
A
B
C
Relative expression of miR-139
CXCR4, CXCL12 relative mRNA expressions
CXCR4, CXCL12 relative protein expressions
p-PLC, PLC relative protein expressions
p-PKC, PKC relative protein expressions
Rho A relative protein expression
MLCK relative protein expression
p-MLC, MLC relative protein expressions
CXCR4
CXCL12
p-PLC
PLC
p-PKC
PKC
p-MLC
Control
IND
TA+L+IND
TA+M+IND
TA+H+IND
CXCR4
CXCL12
p-PLC
PLC
Rho A
MLCK
p-MLC
MLC
β-actin

Fig. 11

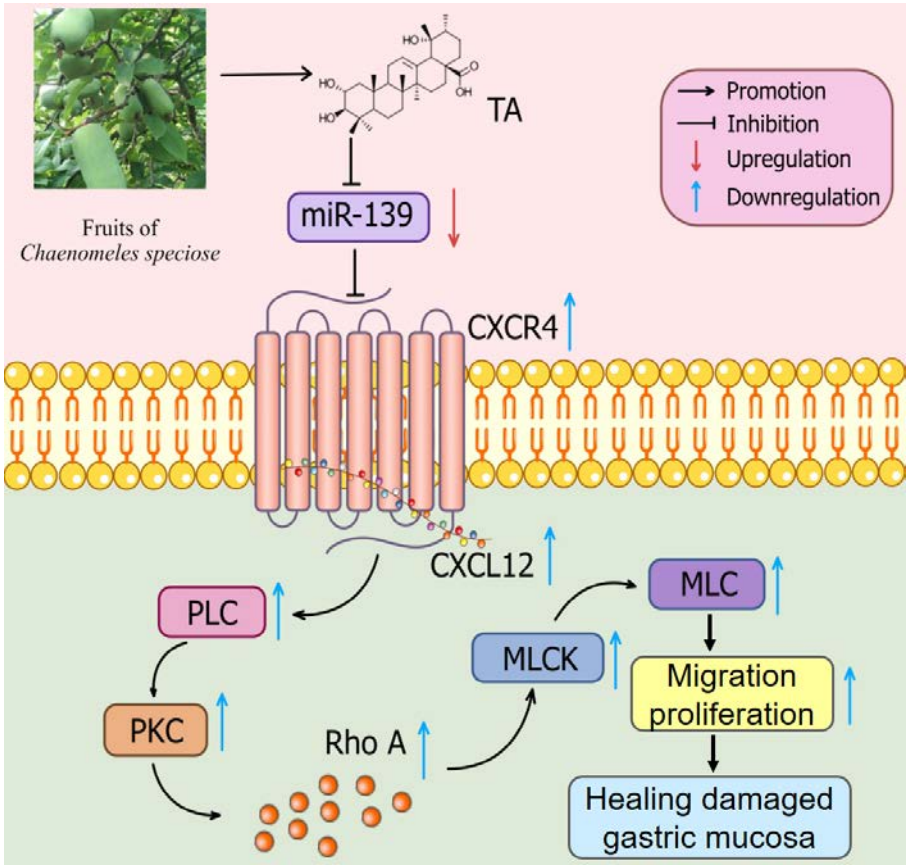
Fruits of
Chaenomeles speciose
TA
Promotion
Inhibition
Upregulation
Downregulation
miR-139
CXCR4
CXCL12
PLC
PKC
Rho A
MLCK
MLC
Migration
proliferation
Healing damaged
gastric mucosa

Fig. 12